Provided for non-commercial research and education use.
Not for reproduction, distribution or commercial use.

VOLUME 243 FEBRUARY 2012 ISSN 0029-5493

Nuclear Engineering and Design

An International Journal devoted to all aspects of Nuclear Fission Energy

Editor-in-Chief: Yassin Hassan
Editors: Jason Chao
Borut Mavko
Dominique Bestion

(Contents continued on back cover)

Available online at www.sciencedirect.com
SciVerse ScienceDirect

Affiliated with the European Nuclear Society (ENS) and with the International Association for Structural Mechanics in Reactor Technology, e.V. (IASMiRT)

This article appeared in a journal published by Elsevier. The attached copy is furnished to the author for internal non-commercial research and education use, including for instruction at the authors institution and sharing with colleagues.

Other uses, including reproduction and distribution, or selling or licensing copies, or posting to personal, institutional or third party websites are prohibited.

In most cases authors are permitted to post their version of the article (e.g. in Word or Tex form) to their personal website or institutional repository. Authors requiring further information regarding Elsevier's archiving and manuscript policies are encouraged to visit:

http://www.elsevier.com/copyright

Author's personal copy

Nuclear Engineering and Design 243 (2012) 214–233

Contents lists available at SciVerse ScienceDirect

Nuclear Engineering and Design

journal homepage: www.elsevier.com/locate/nucengdes

Gas–liquid countercurrent two-phase flow in a PWR hot leg: A comprehensive research review

Deendarlianto[a,b,*], Thomas Höhne[a], Dirk Lucas[a], Karen Vierow[c]

[a] Helmholtz-Zentrum Dresden-Rossendorf e.V., Institute of Safety Research, P.O. Box 510 119, D-01314 Dresden, Germany
[b] Department of Mechanical and Industrial Engineering, Faculty of Engineering, Gadjah Mada University, Jalan Grafika No. 2, Yogyakarta 55281, Indonesia
[c] Department of Nuclear Engineering Texas A&M University, 129 Zachry Engineering Center, 3133 TAMU College Station, TX 77843-3133, USA

ARTICLE INFO

Article history:
Received 25 January 2011
Received in revised form 8 November 2011
Accepted 9 November 2011

ABSTRACT

Research into gas–liquid countercurrent two-phase flow in a model of pressurized water reactor (PWR) hot leg has been carried out over the last several decades. An extensive experimental data base has been accumulated from these studies, leading to the development of phenomenological correlations and scaling parameters of the countercurrent flow limitation (CCFL). However, most of the proposed correlations apply under a relatively narrow range of conditions, generally limited to the test section conditions and/or geometry. Moreover the development of mechanistic models based on the underlying physical processes has been limited. In contrast to this mechanistic form of modelling, the implementation of computational fluid dynamics (CFD) techniques has also been pursued, but the considerable robust three-dimensional (3D) closure relations for this application remain an unachieved goal due to lack of detailed phenomenological knowledge and consequent application of empirical one-dimensional experimental correlations to the multidimensional problem.

This paper presents a comprehensive review of research work on countercurrent gas–liquid two-phase flow in a PWR hot leg and provides direction regarding future research on this topic. In the introductory section, the problems facing current research are described. In the following sections, recent experimental as well as theoretical research achievements are overviewed. In the last section, the problems that remain unsolved are discussed, along with some concluding remarks. It was found that only limited theoretical developments exist in the literature, however highly reliable experimental data are needed to support this effort. Additional work, both analytical and experimental, needs to be carried out on the effects of mass transfer on countercurrent flow limitation to improve the existing correlations and analytical models.

© 2011 Elsevier B.V. All rights reserved.

Contents

* Corresponding author at: Department of Mechanical and Industrial Engineering, Faculty of Engineering, Gadjah Mada University, Jalan Grafika No. 2, Yogyakarta 55281, Indonesia. Tel.: +62 274 521 673; fax: +62 274 521 673.
E-mail address: deendarlianto@ugm.ac.id (Deendarlianto).

0029-5493/$ – see front matter © 2011 Elsevier B.V. All rights reserved.
doi:10.1016/j.nucengdes.2011.11.015

Author's personal copy

1. Introduction

Steam generators in a pressurized water reactor (PWR) nuclear power plant transfer heat from a primary coolant (pressurized water at about 15 MPa) to a secondary coolant (pressurized water/steam at about 7 MPa). The primary coolant water is heated in the core and passes through the steam generators, where it transfers heat to the secondary coolant water to generate steam. The steam then drives a turbine that turns an electric generator. Steam is condensed and returns to the steam generator as feedwater. Hot leg pipes connect the reactor pressure vessel (RPV) and the steam generator (SG), and consist of a combination of horizontal sections, single or multiple elbows, and inclined or vertical sections depending on the manufacturer of the reactor. In the case of the German *Konvoi* PWR, the hot leg consists of a horizontal section, an elbow and an inclined section as shown in Fig. 1. On the other hand, the hot leg of the CANDU reactor is made up of sections of horizontal, vertical, and inclined pipes joined to one another by elbows of varying angles (Kawaji et al., 1989).

In the event of hypothetical accident scenarios in PWR, emergency strategies have to be mapped out, in order to guarantee the reliable removal of decay heat from the reactor core, also in case of component breakdown. One essential passive heat removal mechanism is the reflux cooling mode. This mode can appear for instance during a small break loss-of-coolant-accident (LOCA) or because of loss of residual heat removal (RHR) system during mid loop operation at plant outage after the reactor shutdown.

In the scenario of a loss-of-coolant-accident (LOCA), which is caused by the leakage at any location in the primary circuit, it is considered that the reactor will be depressurized and vaporization will take place, thereby creating steam in the PWR primary side. Should this lead to "reflux condensation", which may be a favourable event progression, the generated steam will flow to the steam generator through the hot leg. This steam will condense in the steam generator and the condensate will flow back through the hot leg to the reactor, resulting in countercurrent steam/water flow. In some scenarios, the success of core cooling depends on the behaviour of this countercurrent flow.

The stratified counter-current flow of steam and condensate is only stable for a certain ranges of steam and water mass flow rates. For a given condensate flow rate, if the steam mass flow rate increases to a certain value, a portion of the condensate will exhibit a partial flow reversal and will be entrained by the steam in the opposite flow direction towards the steam generator. This phenomenon is known as counter-current flow limitation (CCFL) or the onset of "flooding". In case of an additional increase of the steam flow, the condensate is completely blocked and the reflux cooling mode ends. In this situation the cooling of the reactor core from the hot leg is impossible, but may be continued by coolant drained through the cold leg to the downcomer. Fig. 1 illustrates the counter-current flow in the hot leg under reflux condensation conditions.

Over several decades, a number of experimental and theoretical studies of countercurrent gas–liquid two-phase flow have been carried out to understand the fundamental aspect of the flooding mechanism and to prove practical knowledge for the safety design of nuclear reactors. Starting from the pioneering paper of Wallis (1961), extensive CCFL data have been accumulated from experimental studies dealing with a diverse array of conditions. The accumulated data have led to the development of both empirical correlations and analytical models. Bankoff and Lee (1986) reviewed the flooding research in vertical and inclined channels. They presented a summary of the several important parameters on flooding and the available flooding models. They also suggested that more careful experimentation on the parametric dependence is required to investigate the important parameters.

Krishnan (1987) performed a review of the two-phase countercurrent flow in upright pipe elbows as an analogy of the CANDU reactor feeder pipes (hot leg pipe). A total of 4 research papers that were available in the year of 1986 (Siddiqui et al., Wan and Krishnan, Wan, and Ardron and Banerjee) are included in his review papers. Krishnan compared the onset of flooding data obtained from the experimental and the numerical studies proposed by those authors, and discussed the possible sources of the unexpected results which were revealed from the above investigations. Finally he recommended that new experiments are also needed to provide information on the mechanism of flooding. The points above highlight the importance of knowing the current status of research in this field to better identify the direction of future research

The objective of the present paper is to summarize the recent developments in research, addressing the behaviour of the counter-current flow in a complex piping system as the analogy of the PWR hot leg. Both experimental and modelling efforts are considered. In the present review article, experimental studies on counter-current flow in a PWR hot leg are intensively reviewed firstly. All effective possible research subjects were classified generally according to the elbow configurations (single or multiple). Brief information on the flow pattern, void fraction, CCFL characteristics and the involved mechanisms are given. In the second part of this paper, the analytical developments in this field are presented. In addition the use of CFD to explore three dimensional (3D) phenomena around CCFL, as a new research area, is reviewed briefly. Finally, the scientific reasons why we have had limited success in the mechanistic modelling of CCFL and the future research directions for this important area are described.

2. Basic terminologies

The basic definitions in counter-current air–water two-phase flow have been given by Celata et al. (1989). Those include the terminologies of the onset of flooding and zero penetration point. For the case of the countercurrent flow in a model PWR hot leg, the detail terminologies and flow regime have been given by Deendarlianto et al. (2008), and only the main features are presented here.

In their experimental work, the liquid flow rate was kept constant, and the air flow rate was increased and decreased in small increments and decrements respectively. Air–water data in a particular test section are used for illustrative purposes. The trends and values will differ for steam–water data under PWR hot leg conditions. Two tanks were used to simulate the reactor pressure vessel (RPV) simulator and the steam generator (SG) separator in the actual German PWR. In the experiment, the air was injected in the RPV simulator and flowed through the test section to the SG separator, from which it was released to the atmosphere. The water from the feed water pump was injected in the SG separator, from where it could flow in counter-current mode to the air flow through the test section to the RPV simulator.

Author's personal copy

Nomenclature

A	area or interfacial area density (m^2)
Bo	Bond number (−)
C	constant in Eqs. (2) and (7) (−)
C_D	drag coefficient (−)
C_p	specific heat of liquid at constant pressure (J/(kg K))
D	inner pipe diameter (m)
D^*	dimensionless number of pipe inner diameter (−)
D_d	droplet diameter (m)
D_H	hydraulic diameter (m)
f_i	interfacial friction factors (−)
f_{wk}	phase-wall friction factors (−)
g	gravitational acceleration (m/s^2)
h_{LG}	specific enthalpy (J/kg)
J_K	phase superficial velocity (m/s)
$J_{L,D}$	discharged superficial liquid velocity (m/s)
J_K^*	Wallis dimensionless number of superficial velocity (−)
Ku_G	Kutateledze dimensionless number of the gas phase (−)
L	characteristic length (m)
L_H	length of horizontal leg (m)
I	length of riser (m)
m	constant in Eq. (2) (−)
m_G	gas mass flow rate (kg/s)
$m_{L,D}$	discharged liquid flow rate (kg/s)
R_T	thermodynamic ratio (−)
$\tilde{S}_i$	normalized of interface width (−)
T_L	liquid temperature (K)
T_{sat}	saturation temperature (K)
u_K	phase mean velocity (m/s)
We	Weber number (−)

Greek letters

α	gas void fraction (−)
α_G	void fraction at the onset of slugging at the hydraulic jump near the pipe bend (−)
β	upward inclination angle from horizontal (degree)
θ	downward inclination angle of the lower leg to the horizontal
ρ_k	liquid and gas density (kg/m^3)
$\tau_{L,G}$	wall shear stresses of the gas and liquid onto the free surface
τ_{wk}	wall shear stress (N/m^2)
τ_i	interfacial shear stress (N/m^2)

List of abbreviations

AIAD	algebraic interfacial area density
CCFL	counter-current flow limitation
CFD	computational fluid dynamics
FZK	Forschungszentrum Karlsruhe
HZDR	Helmholtz-Zentrum Dresden Rossendorf
KNSPP	Korean standard nuclear power plant
LOCA	loss-of-coolant-accident
PWR	pressurized water reactor
RPV	reactor pressure vessel
SG	steam generator
SST	shear stress transport
UPTF	upper plenum test facility
VOF	volume of fluid
WENKA	Wasser und Entrainment Kanal
ZP	zero-liquid penetration

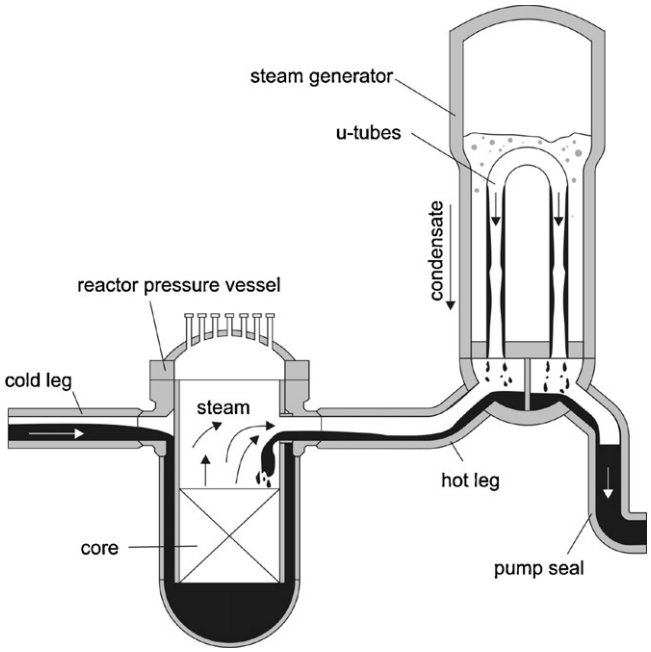

Fig. 1. *Konvoi* German PWR piping configuration and reflux condensation flow paths (Seidel et al., 2010).

For small gas flow rate, the liquid film flows counter currently with the gas phase in hot leg channel. The pressure difference inside the test section is still low, and slightly increases with the air mass flow rate. This regime is defined as the stable countercurrent flow. As the gas flow rate (m_G) is gradually increased, thus, there is the maximum gas flow rate in which the down-flowing water mass flow rate ($m_{L,D}$) in reactor pressure vessel is equal to the inlet water mass flow rate. This point is defined as the onset of flooding or counter-current flow limitation (CCFL) as shown in Fig. 2. With further increasing of the air mass flow rate, the down-flowing water mass flow rate ($m_{L,D}$) in RPV simulator is close to zero. This point corresponds to the zero liquid penetration (ZP). The region between the CCFL and ZP is defined as partial delivery region. In turn, when the gas flow rate is decreased, a point is reached where a fully counter-current gas–liquid two-phase flow is established. This is known as the deflooding point.

"Scaling" in general encompasses all differences existing between a real full-size industrial plant and a corresponding

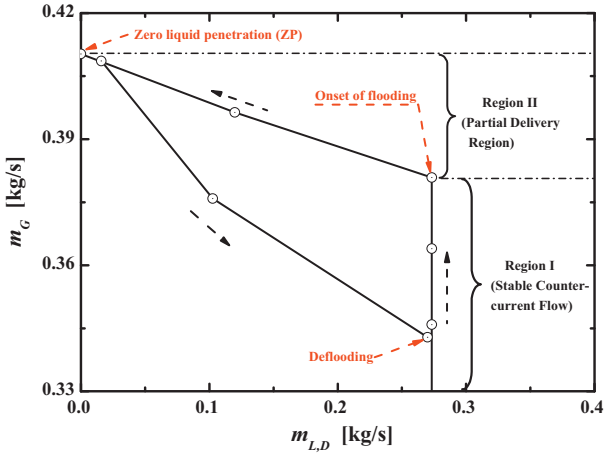

Fig. 2. Terminologies in countercurrent gas–liquid two-phase flow in a model of PWR hot leg presented by Deendarlianto et al. (2008).

Author's personal copy

experimental facility. An experiment may differ in geometric dimensions and shape or event in the applied test facility (Glaeser and Karwat, 1993). Determination of the parameters needed to be scaled to the proper dimensions and magnitude to best represent the test channels is one of the purpose of the countercurrent flow studies. A number of useful empirical correlations by various investigators have been proposed over the past several decades for this purpose. Careful implementation of the suitable related dimensionless parameters, which requires good understanding of the experimental phenomenon, is necessary. In the case of vertical channels, two important dimensionless parameters have emerged: the Wallis parameter and Kutateladze number (Bankoff and Lee, 1986).

Wallis (1961) proposed the dimensionless parameter, J_K^*, in terms of the gas and liquid superficial velocities to correlate the gas velocity at flooding in vertical tubes. This parameter represents the ratio of inertial force to hydrostatic force, and is defined as follows:

$$J_K^* = J_K \sqrt{\frac{\rho_K}{gL(\rho_L - \rho_G)}} \tag{1}$$

where the subscript K indicates gas and liquid phases, ρ the density, g the acceleration of gravity, and L the characteristic length. In the case of circular tube, the length scale should be the flow channel inner diameter. Using this parameter Wallis proposed the following correlation for the CCFL as,

$$(J_G^*)^{1/2} + m(J_L^*)^{1/2} = C \tag{2}$$

Several investigators (Pushkina and Sorokin, 1969; Alekseev et al., 1972) suggested a correlation using the surface tension, σ, instead of inner pipe diameter for defining the suitable dimensionless quantity. The correlation is incorporated in the Kutateladze number. It was derived from consideration of the stability of the liquid film or from the gas flow needed to suspend the largest stable liquid drop (Levy, 1999), and is defined as follows.

$$Ku_K^* = \frac{J_K \rho_K^{1/2}}{[g\sigma(\rho_L - \rho_G)]^{1/4}} \tag{3}$$

In comparing both dimensionless numbers (Eqs. (1) and (3)), it can be seen that both of them do not involve the viscosity of the fluids. Instead the different presence of the characteristic length in the Wallis parameter and the surface tension in the Kutateladze number is the main difference. The relation between the two dimensionless numbers can be made as follows.

$$Ku_K^* = J_K^*(D^*)^{1/2} \tag{4}$$

where D^* is the square root of the Bond number, Bo, and is defined as below.

$$Bo^{1/2} = D^* = D\left[\frac{(\rho_L - \rho_G)g}{\sigma}\right]^{1/2} \tag{5}$$

In the case of vertical pipe, interpolation between Wallis and Kutateladze dimensionless numbers have been suggested to resolve the role of tube diameter (Levy, 1999). The Wallis parameter is valid for the small inner pipe diameter and the Kutateladze for the large one. Wallis and Makkenchery (1974) noted that the transition between small and large diameter tubes occurs for a Bond number of 40.

Zapke and Kroger (2000) present a more recent evaluation of dimensionless parameters for correlating flooding data. Through a discussion of properties and flow conditions that could affect flooding, they show that the Froude number (Fr) and the Ohnesorge (Oh_L) number best reproduce air–water flooding data in vertical straight tubes. The Froude number is a ratio of inertial to buoyancy forces while the Ohnesorge number is a ratio of liquid viscous to surface tension properties.

$$Fr = \frac{\rho_L J_L^2}{gD_H(\rho_L - \rho_G)} \tag{6}$$

$$Oh_L = \sqrt{\frac{\mu_L^2}{\rho_L D_H \sigma}} \tag{7}$$

where D_H is the hydraulic diameter, and μ the liquid viscosity. The gas Froude number was found to be a function of the liquid Froude number to the 0.2 power multiplied by the liquid Ohnesorge number to the 0.3 power. While the coefficients change, these parameters reflect well the data for flooding in large diameter tubes (Solmos et al., 2008).

All of the above parameters were derived for CCFL in straight vertical tubes, without mass exchange between the phases. The hot leg phenomena differ in important manners and therefore the CCFL trigger mechanism is different. Firstly, in a vertical tube with uninterrupted flow, momentum exchange at the phase interface dictates the CCFL trigger. The gas phase and the liquid phase are in contact only at the continuous interface. The CCFL is thought to be due to a surface instability. In the hot leg, the flow experiences an interruption at a bend, thereby causing secondary flows within each phase and interfacial interactions at beyond just a continuous interface. Secondly, when vapor is being condensed or generated, the mass flow rate of either phase is a variable with location in the flow channel. Condensation will reduce the mass flow rate and drastically decrease the amount of momentum that the vapour phase is able to transfer to the liquid phase. Consequently, the force ratios above are not expected to predict the onset of CCFL in the hot leg. The correlations are being used in situations beyond those they were intended for. As will be seen, the nature of the flow channel bend and other flow parameters are introduced into many of the empirical correlations for the hot leg flooding.

3. Comprehensive overview of the countercurrent flow studies in a model of PWR hot leg

In this section, a comprehensive review on the studies of counter-current flow in a model PWR hot leg is presented. There is a wealth of information in the journals and texts regarding those topics. The literature can be broken down into two categories: experimental investigation and theoretical analysis.

3.1. Experimental investigations

Presented here is a review of the literatures discussing on the experimental works on CCFL, flooding mechanisms, and correlations for predicting CCFL in a complex piping system that represents the pipe configuration of the PWR hot leg in a nuclear reactor. From the view point of application, the review of experimental works is broken down into two categories: single elbow and multiple elbows.

3.1.1. Single elbow

Table 1 shows the summary of the available literatures on the countercurrent flow using a single elbow in a model of PWR hot leg. In the table the summary includes both experimental and analytical works, and is listed in chronological order. The latest studies have been included in this table. The definitions of the geometries of the channel used in Table 1 are given in Fig. 3.

Table 1 indicates that there are many more studies on countercurrent flow in a complex piping system using the air–water as test fluids, whereas relatively fewer studies deal with steam–water (Ohnuki, 1986; Wan, 1986; Mayinger et al., 1993; Glaeser and Karwat, 1993; Lucas et al., 2008). The possible reason is due to the

Author's personal copy

Table 1
Summary of investigations on the counter-current flow study in a model of PWR hot leg using single elbow.

Researchers/year	Experimental conditions	Practical analogy	Analytical studies	Experimental targets	Remarks
Richter et al. (1978)	– Air–water test – Circular tube (ID = 8 in., L_H = 3 ft, β = 45)	1/30th scale down of PWR hot leg	N/A	CCFL	Flooding correlation by using Wallis parameters' should be appropriate to correlate the limitation of reverse flow of water into the steam generator
Siddiqui et al. (1986)	– Air–water test – Circular tube (36.5 mm < D < 47 mm; 24 < L_H/D < 95; β = 90°; 0 mm < R < 300 mm)	Simplified model of CANDU PWR hot leg	N/A	CCFL, geometrical effect studies on CCFL (channel configuration), void fraction, complete carry up	Flooding is caused by slugging at the hydraulic jump in the lower leg of elbow close to the bend, and the instability criterion on it was proposed (Eq. (8))
Ardron and Banerjee (1986)	(Analytical validation using the data of Siddiqui et al., 1986)	Simplified model of CANDU PWR hot leg	**Analytical studies** (one-dimensional stratified two-fluid model/free out fall assumption)	N/A	A theoretical model was developed on the basis of experimental assumptions, and an empirical CCFL correlation was proposed (Eq. (21))
Ohnuki (1986)	– Air–water & steam–water tests – Circular tube (26 mm < D < 76 mm; 10 mm < L_H < 400 mm; 40° < β < 45°; 38 mm < I < 600 mm; 20 mm < liquid head < 100 mm)		**Analytical studies** (Envelope theory to solve momentum balance equations under separated counter-current flow)	Flow Pattern, geometrical and working fluid effects on CCFL	– A new empirical flooding correlation was proposed (Eq. (9)) – The geometrical and working fluids effects on CCFL were clarified
Weiss and Hertlein (1988)	– Steam–water – Circular tube (D = 750 mm, β = 50°) (UPTF exp. Model, see Fig. 4)	Full scale of German PWR hot leg	N/A	CCFL	New steam–water CCFL data on a full scale German PWR hot leg were provided
Ohnuki et al. (1988)	– Air–water test – Circular tube (a) Normal model (D = 25.4 mm; L_H = 260 mm; β = 50°; I = 60 mm; R = 77.5 mm) (b) UPTF exp. model, but the dimension was the same as the normal model	Model of German PWR hot leg (UPTF)	**Analytical studies** (The using of the envelope theory to solve momentum balance equations)	Flow Pattern, Pressure effect on CCFL, void fraction measurements using Gamma-densitometers	– The proposed equation (Eq. (9)) based on small scale experiments could not be extrapolated to real dimension of PWR – The degree of the shift was not affected by the change of pressure (0.3 MPa → 1.5 MPa)
Tehrani et al. (1990), Gardner (1988)	– Air–water test – Circular tube (D = 84 mm, L_H = 588 mm, and β = 50°)	(1/9th scale of Sizewell 'B'** PWR)	N/A	CCFL (flooding & deflooding), Pressure gradient	Hysteresis between flooding and deflooding appeared
Kawaji et al. (1989, 1991)	– Air–water test – Circular tube (D = 51 mm, and five variations of L_H, β, and I)		**Semi analytical model** (Slugging and liquid carryover)	Geometric effects on CCFL	The observed flooding mechanisms are the slugging and droplet entrainment/carryover. A Weber number based on local liquid velocity was used to determine the droplet size required in the droplet entrainment/carryover model

Table 1 (*Continued*)

Researchers/year	Experimental conditions	Practical analogy	Analytical studies	Experimental targets	Remarks
Ohnuki et al. (1992)	(The experimental data from the open literatures under various conditions of scale, pressures, and fluid combinations)		Development of the interfacial friction model for two-fluid model for PWR hot leg	N/A	– The model is mainly composed of the interfacial friction model in countercurrent flow both for stratified and slug flow regimes – The present interfacial friction model is valid for the CCFL with the range of diameter between 0.025 & 0.75 m (air–water & steam–water)
Geweke et al. (1992)	– Air–water test – Circular tube (D = 65 mm; L_H = 565 mm and 648 mm; β = 50°)	Model of 1:11.5 scale of German PWR hot leg	**Analytical studies** (one-dimensional stratified two-fluid model/envelope theory)	Flooding mechanism, CCFL	Flow mechanisms in the countercurrent gas–liquid two-phase flow were observed, and new CCFL data were provided
Glaeser (1992)	N/A	Model of full scale of German PWR hot leg	Analytical work on the determination of the scaling parameter of CCFL in a PWR hot leg	N/A	There is only the Wallis correlation applicable to horizontal countercurrent flow. There is no change to the Kutateladze number criterion in contrast to vertical countercurrent flow
Mayinger et al. (1993)	– Steam–water test – Circular tube (D = 750 mm, β = 50°) – System pressure: 0.3 MPa and 1.5 MPa	Model of full scale of German PWR hot leg	Calculation of the water level in PWR hot leg by using ATHLET system code	Flow pattern, CCFL, measurement of water level in PWR hot leg	– The Wallis parameter adequately accounts for pressure effect on CCFL – The CCFL in the hot leg occurs at the bend part of the hot leg, because of the accumulation of water reaches the maximum there
Glaeser and Karwat (1993)	– Steam–water test – Circular tube (D = 750 mm, β = 50°) – System pressure: 0.3 MPa and 1.5 MPa	Model of full scale of German PWR hot leg	N/A	CCFL	The flooding data can be described by a Wallis-type equation for different sizes of test facilities (Eq. (10))
De Bertodano (1994)	(The experimental data from the Ohnuki et al. (1988) was used to validate the developed analytical model)	General hot leg PWR	**Analytical studies** (momentum balance equations combined with slugging criterion of Kelvin–Helmholtz)	N/A	The hydraulic jump observed in the small scale experiment does not occur at full scale, and a new empirical correlation was derived from the analytical study (Eq. (23))
Wongwises (1994, 1996a)	– Air–water test – Circular tube (D = 64 mm; $8.7 < L_H/D < 44$; $50° < \beta < 90°$; I = 1215 mm; R = 60 mm)		N/A	Flow Pattern, CCFL, void fraction, zero liquid penetration	Flooding curve is divided into three regions, in each of which the mechanism of flooding is different. Those mechanisms are dependent on the water flow rate
Wang and Mayinger (1995)	– Steam–water – Circular tube (D = 750 mm, β = 50°) (The experimental data of UPTF were used to validate the CFD)	Full scale of PWR hot leg of UPTF experimental model	**CFD modelling (2D)** (using FLOW 3D of the two-fluid model)	N/A	The simulation was successfully implemented to the Test 11 of UPTF
Stevanovic and Studovic (1995)	The experimental data from the open literature were used to validate the model		**Analytical studies** (one-dimensional stratified two-fluid model/free out fall assumption)	N/A	– The model has been verified for the various experimental data – The interfacial transfer is very crucial for the accurate simulations

Author's personal copy

Author's personal copy

Table 1 (*Continued*)

Researchers/year	Experimental conditions	Practical analogy	Analytical studies	Experimental targets	Remarks
Wongwises (1996b)	– Air–water test – Circular tube (D = 64 mm; 8.7 < L_H/D < 44; 50° < β < 90°; I = 1215 mm; R = 60 mm)		**Analytical studies** (one-dimensional stratified two-fluid model/free-out fall assumption)	Flow pattern, geometric effects on CCFL, void fraction, zero liquid penetration	The geometrical effect on CCFL was clarified, and a slight modification of the Ardron and Banerjee (1986) model on the basis of void fraction measurement was proposed
Kang et al. (1999)	– Air–water test – Circular tube (8 number of test section includes 1/650 & 1/3675 vol. reduction ratio of Korean standard PWR hot leg) (D = 80 mm and 40 mm; 12 < L_H/D < 85; I = 0 mm, 623 mm, 648 mm; β = 0° & 35°)	Model of PWR hot leg of Korean Standard (KSNPP, Ulchin 3 & 4)	N/A	Flooding mechanisms, geometric effects on CCFL	– Experimental CCFL correlation was proposed (Eq. (14)) – CCFL occurred at much lower when the lower part of the horizontal pipe was initially filled with stagnant water – The flooding mechanisms were similar to the result from Wongwises (1996a)
Chun et al. (1999)	– Air–water test – Circular tube (8 numbers of test section includes 1/650 & 1/3675 vol. reduction ratio of Korean standard PWR hot leg) (D = 80 mm and 40 mm; 12 < L_H/D < 85; 0 mm < I < 648 mm; β = 0° & 35°)	Model of PWR hot leg of Korean Standard (KSNPP, Ulchin 3 & 4)	N/A	Flooding mechanisms, geometric effects on CCFL	The results are the same as those of Kang et al. (1999)
Wan and Krishnan (1986)	– Air–water test – Circular tube (D = 51 mm, β = 90°, and the inclination of the horizontal leg is +0.35° to −0.25°)	Simplified model of CANDU PWR hot leg	N/A	Flow pattern, CCFL (inclination effect)	– Flooding mechanism was slugging – The flooding limit is sensitive to small change (≤1°) in the inclination angle
Wan (1986)	– Steam–water test – Circular tube (D = 51 mm; β = 90°) – subcooled water: ΔT_{sub} < 6 °C	Simplified model of CANDU PWR	N/A	Flow pattern, CCFL	Flooding regime map was proposed, and the effect of subcooled water was clarified
Geffraye et al. (1995)	– Air–water test – Circular tube (4 different test section were used)	– Model of French PWR hot leg – 1/100 scale down of the French 3-loop PWR (BETHSY geometry)	N/A	CCFL and zero liquid penetration	The scattering of the flooding data on Wallis parameters is around 50%, whereas the scattering on the Kutateladze parameters is 300%
Kim and No (2002)			Development of empirical correlation by using the experimental data base in open literature	N/A	New CCFL correlation is derived (Eq. (15)), which shows the L/D effect. The present correlation agrees well with the database within the prediction error of 8.7%
Gargallo et al. (2005)	– Air–water test – Rectangular cross section (90 mm × 110 mm, L = 440 mm)	German PWR	CCFL and flow reversal criteria	CCFL and flow reversal criteria	The hydraulic jump is the initiator for a water flow reversal
Navarro (2005)	– Air–water test – Circular tube (36 mm < D < 54 mm; 0.1 m < L_H < 0.8 m; 30° < β < 90°; 0.1 m < I < 0.35 m)		N/A	Geometric effects on CCFL, zero liquid penetration, pressure gradient, void fraction	– The hydraulic jump was only observed in the test configuration with β = 90° at low liquid flow rate – The effects of the channels sizes were clarified – Empirical CCFL correlation was proposed (Eq. (16))

Table 1 (*Continued*)

Researchers/year	Experimental conditions	Practical analogy	Analytical studies	Experimental targets	Remarks
Minami et al. (2008a,b)	– Air–water test – Rectangular cross section (150 mm × 10 mm, L_H = 1240 mm, R = 240 mm, and β = 50°)	1/5th of the scale down diameter of PWR hot leg	**1. Analytical model (1D)** (The using of the envelope theory to solve momentum balance equations) **2. CFD modelling (3D)** (Two-fluid model using FLUENT6.3.26)	Flow pattern, CCFL, film thickness measurement	– Flow pattern in the elbow and inclined section were strongly affected by those in the horizontal section – The transition line from stratified flow to wavy flow is close to the CCFL correlation, and can be expressed by a Wallis-type CCFL correlation – The void fraction measurement results along the rectangular cross section were provided (Table 2). – The 1D analytical model and CFD calculation agree well with the experimental data (Minami et al., 2008b)
Deendarlianto et al. (2008), Vallée et al. (2008, 2009)	– Air–water – Rectangular channel (250 mm × 50 mm), L_H = 2120 mm, R = 250 mm, β = 50°	1/3rd of the diameter of German *Konvoi* PWR hot leg	N/A	Flow pattern, CCFL	New air–water CCFL data of rectangular channel for CFD code validation were provided, and the fundamental effect were clarified (hysteresis, pressure, and liquid mass flow)
Lucas et al. (2008)	– Steam–water – Rectangular channel (250 mm × 50 mm), L_H = 2120 mm, R = 250 mm, β = 50°	1/3rd of the diameter of German *Konvoi* PWR hot leg	N/A	Flow pattern, CCFL	New steam–water CCFL data of rectangular channel of PWR hot leg for CFD code validation were provided, and the difficulty in experimental running of steam–water were clarified
Murase et al. (2009), Minami et al. (2009), Utanohara et al. (2009)	Air–water – Circular tube (D = 50 mm, L_H = 430 mm, l = 60 mm & β = 50°)	1/15th of the diameter of PWR hot leg	**CFD modelling (3D)** (VOF & two-fluid model using FLUENT6.3.26)	Flow pattern, CCFL	It is better to use the two-fluid model with suitable interface friction correlations than the VOF model at least in the case of large size meshes to calculated global behaviour
Kinoshita et al. (2009)	Steam–water & Air–water tests	1/15th of the diameter of PWR hot leg & real diameter of hot leg	**CFD modelling (3D)** (Two-fluid model using FLUENT6.3.26)	– Air–water data refers to the above papers. – Steam–water data refers to UPTF	Due to the calculation meshes were relatively large & the generation and growth of waves could not be calculated
Minami et al. (2010a,b)	– Air–water test – Circular tube (D = 50 mm, L_H = 430 mm, l = 60 mm & β = 50°)	1/15th scale down of the diameter of PWR hot leg	**CFD modelling (3D)** (Modelling of two-fluid & k-ε model using FLUENT6.3.26).	Flow pattern & CCFL	– Flow patterns in the elbow and the inclined section were strongly affected by those in the horizontal section – The selected combination of interfacial friction coefficient can be utilized for 3D two-fluid model of CCFL in hot leg geometry
Nariai et al. (2010)	Air–water & Air-Glycerol solution with difference concentration – Circular tube (D = 50 mm, L_H = 430 mm, l = 60 mm & β = 50°)	1/15th of the diameter of PWR hot leg	**Analytical model** (1D momentum balance for stratified flow).	CCFL (liquid properties effect), water level measurement	– The interfacial force must not depend on the liquid viscosity and surface tension. – The CCFL predicted by 1D momentum balance agree well with the measured exp. data
Deendarlianto et al. (2010)	Experimental data of Deendarlianto et al., 2008 were used to validate the CFD modelling	1/3rd of the diameter of German *Konvoi* hot leg PWR	**3D CFD modelling** (Using the AIAD model)	N/A	The CFD model is in agreement with the exp. data
Vallée et al. (in press)	Air–water	General PWR hot leg model	Scaling parameter studies	N/A	The channel height is the characteristic length to be applied to the Wallis parameter for channel with rectangular cross section

Author's personal copy

Author's personal copy

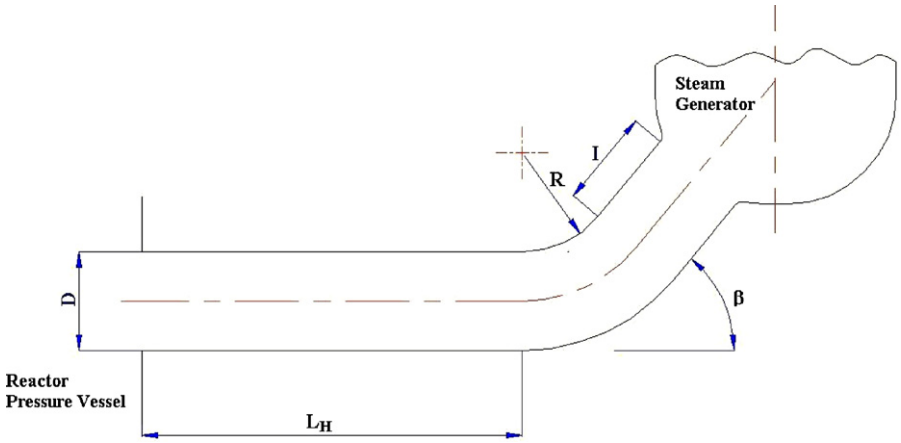

Fig. 3. Idealization of the channel configurations of the countercurrent gas–liquid two-phase flow in a complex piping system using a single elbow.

complexity of phenomenon in the steam–water experiment caused by the condensation effects. The available studies are described, respectively, in the following.

One of the earliest works was performed by Richter et al. (1978). They investigated the CCFL in a 1/30th scale down of PWR hot leg. The inner pipe diameter was 203 mm. A single elbow was used to connect the horizontal pipe to an inclined pipe with the inclination angle of 45°. They noticed that the gas flow required to produce flooding is much smaller than that for a simple vertical pipe. The CCFL correlation by using Wallis parameters' should be appropriate to correlate the limitation of the reverse flow of water into the steam generator, in which the coefficients of m and C are 1.0 and 0.7 respectively.

Siddiqui et al. (1986) conducted a flooding study in an elbow between a vertical and horizontal or near horizontal pipe experimentally. This configuration represents the idealization of the feeder/hot leg pipes in CANDU pressurized heavy water reactor. The air and water were employed as the working fluids. The CCFL data were presented in terms of phases Wallis parameters. They found that the CCFL curves depend on the inner tube diameter, the length and inclination of the lower leg of the elbow, and radius of the curvature of the bend. This indicates that the Wallis parameter is not able to correlate the CCFL data of different inner pipe diameter, although the inner pipe diameter is included in this parameter. From the visual observation, they found that flooding to be caused of by slugging at the hydraulic jump that formed in the lower leg of the elbow close to the bend, and occurs according to the below equation.

$$J_G^* = 0.2\alpha_G^{3/2} \tag{8}$$

where α_G is the local gas void fraction at the crest of the hydraulic jump.

Ohnuki (1986) conducted a CCFL experimental series in a small scale PWR hot leg with air–water and saturated steam–water fluid combinations. Here Ohnuki varied the most important geometrical aspects of the hot leg: the inner pipe diameter, the length of the horizontal leg, shape of the upper exit riser, and water head in the plenum to which the inclined tube is connected. As a basis of the comparison, similar experiments in an inclined pipe (without horizontal part) were also conducted. The CCFL data was also presented in terms of the phases Wallis parameters'. Ohnuki found that the CCFL curve is independent of the combination of the working fluids (saturated steam–water and air–water). This conclusion is reasonable for fluids in thermal equilibrium because there is no mass transfer effect and the saturated steam is able to transfer momentum to water along the length of the test section similar to the air-to-water momentum transfer. The length of the horizontal part, length of the riser, and shape of upper exit has a significant effect on the CCFL. Moreover there was no effect of the inner pipe diameter and the shape of the bend on the CCFL curve. For a common outlet of hot leg (with circular cross-section), Ohnuki concluded that a linear relationship expressed in Wallis parameter can be applied as a scaling parameter to the CCFL data under atmospheric pressure, as long as the flow is not an unsteady flow. Finally he proposed a value of 0.75 for the constant of m and the following function for C:

$$C = \ln\left\{\left(\frac{L_H}{D}\right)\left(\frac{1}{I}\right)\right\}^{-0.066} + 0.88 \tag{9}$$

where I is the length of the inclined riser.

The objective of the investigation in the upper plenum test facility (UPTF) was to determine the limit of countercurrent flow of saturated steam–water in 1:1 of a German PWR hot leg. The inner pipe diameter was 750 mm. The idealization of the UPTF experimental configuration is shown in Fig. 4. As shown in the figure, a secondary pipe to simulate the emergency core cooling (ECC) port in a real nuclear reactor also called *Hutze*, was installed in the horizontal part of the test pipe. The experiments were done under two system pressures, 3 bars and 15 bars. The CCFL data were plotted in terms of phases Wallis parameters' J_K^*, in which the length scale is calculated from the hydraulic diameter of the effective flow area at the region with *Hutze*.

The results were reported in series by Weiss and Hertlein (1988), Weiss et al. (1992), Mayinger et al. (1993), and Glaeser and Karwat (1993). Experimental results showed that the water run-back to the test vessel decreases as the steam flow increases. The data at the two system pressures are in close agreement, and indicate that the Wallis parameter adequately accounts for this effect (Mayinger et al., 1993). Mayinger et al. also compared their CCFL data with the available experimental correlations derived from sub-scale experiments from Richter et al. and Ohnuki. The Richter correlation passes through the UPTF data, which is obviously due to the similar configuration of the flow channel.

Later, the analysis of the UPTF experimental results was extended by Glaeser and Karwat (1993). They reported that the CCFL data can be correlated by a Wallis-type equation as follows

$$(J_G^*)^{1/2} + m(J_L^*)^{1/2} = C_1 = C_2(\sin\ 40^\circ) \tag{10}$$

with $m = 0.7–1.0$ and $C_1 = 0.61–0.75$. This is in contrast of the conclusions of Levy (1999) for straight vertical tubes. Here the Wallis parameter is used for smaller diameter tubes, where the tube diameter effect is important.

Ohnuki et al. (1988) extended their previous work in order to assess the possibility of applying Eq. (9) as a scaling parameter for the actual size of PWR hot leg. Two types of pipe configurations

Author's personal copy

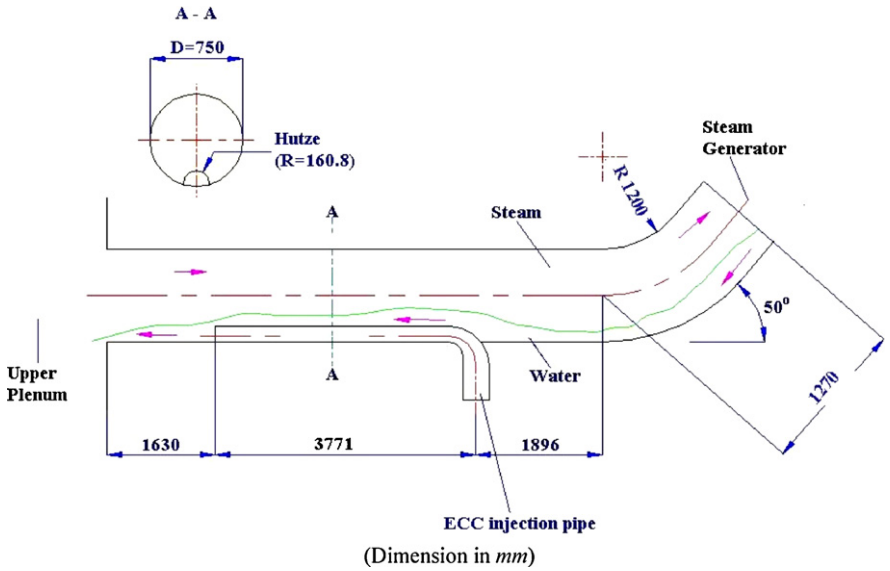

Fig. 4. Test channel configurations of the UPTF experiments (Wang and Mayinger, 1995) (dimension in *mm*).

were adopted in this study: type A having a test section without ECC injection/*Hutze* and type B having a test section using the *Hutze* as used in the UPTF experiment. The inner pipe diameter was 25.4 mm for both test sections. The other dimensions for types A and B were determined by selecting approximately the same value of the ratio between: (a) length of horizontal pipe to inner pipe diameter, (b) length of horizontal pipe to that of inclined riser, and (c) the height of *Hutze* to inner pipe diameter as those in the UPTF experiment. They found that when using the superficial velocity and length scale in the Wallis parameter (J_K^*) estimated by the flow area and the diameter of the flow path at the region without *Hutze*, Eq. (9) over-predicts the UPTF data. In order to eliminate the effect of *Hutze*, they modified the flow area and diameter on J_K^* by using combinations of the hydraulic cross sectional area and hydraulic diameter of the region of *Hutze*. Finally, they noticed that the Wallis parameter has the capability to compensate for the scale effect when the inner pipe diameter is more than 0.203 m and on the pressure effects of up to 1.5 MPa. However they were not able to explain these findings in their study. It is interesting to note that it has a contradicting effect to that of the scaling factor of the CCFL in vertical pipes, in which the Wallis parameter is valid only for the small inner pipe diameter as noted by Wallis and Makkenchery (1974).

To better understand the parameters which may influence the CCFL, an experiment has been carried out by Geffraye et al. (1995) under the MHYRESA experimental program. The various test sections included two types of hot leg geometry, three diameters from 0.075 m to 0.351 m and allowed for the investigation of the geometrical effect on the CCFL. The CCFL was determined by two methods. Those are determined when the pressure drop above the flooding locus shows a sudden increase and the liquid down-flow rate is smaller than the feedwater flow rate. From the visual observation, they noticed that the CCFL never takes place at the SG inlet plenum. The CCFL data were compared to available experimental data and empirical correlations, whereas the attention was focused on the zero liquid penetration point. The comparison was made by using the Wallis parameter and Kutateladze number. Results showed that the CCFL point seems to be rather better described by the Wallis parameter in the range of 0.0254–0.75 m. The scattering on the Wallis parameter is around 50%, whereas it on Kutateladze parameter is around 300%. However no general trend can be found when looking to the smaller scale data. Moreover they pointed out also that it seem more reasonable to accept that the CCFL in a hot leg will remain a phenomenon which cannot be predicted with a high accuracy.

Wan and Krishnan (1986) investigated the air–water flooding in a 90° elbow with a slightly inclined lower leg. The inclination angle of the lower leg ranged from +0.35° to −0.25°. The inner pipe diameter was 51 mm. The purpose of their work was to investigate thoroughly the effect of small inclinations of the lower leg of an elbow on flooding behaviour in air–water flow. In general, their experimental results confirmed the observation of Siddiqui et al. (1986). At low liquid flow rate, the flooding occurred as a result of slugging at the crest of a hydraulic jump in the horizontal leg. On the other hand, at high liquid flow rates corresponding to $J_L^{*1/2} > 0.5$, no hydraulic jump was observed; flooding occurred due to the slug formation at the end of the horizontal leg which travelled upstream to water carry-up through the vertical leg.

Wan (1986) used the same experimental apparatus of that of Wan and Krishnan to investigate the effect of interface mass transfer during the countercurrent steam–water flow. The subcooling of the water inlet was up to 6 °C. The CCFL data was presented in terms of Wallis parameters'. Three (3) flow regimes during the countercurrent steam–water flow were observed. The qualitative map of those flow regimes is shown in Fig. 5. Those are explained as follows.

1. Regime I is a region of steady counter-current flow in which the phases are stratified in the horizontal leg.
2. In regime II, the occurrence of slugging is accompanied by partial or total carry over of the injected water. In the figure, the boundary between regimes I and II is marked as boundary #1. Here the formation of a slug in the horizontal leg was taken as the inception of flooding. In the case of atmospheric condition, it is appeared in the range of $J_L^{*1/2} < 0.5$. In this range, the effect of water inlet subcooling was minor.
3. Regime III is a complete penetration of water into the elbow. Here, an oscillatory water column occurred in the vertical leg without any carryover of injected water.

In Fig. 5, the boundaries between regimes I and III, and regimes II and III are respectively marked as boundary #2 and boundary #3. The CCFL curves are also expressed by those boundaries. The CCFL curves are dependent upon the inlet water sub-cooling. The

Author's personal copy

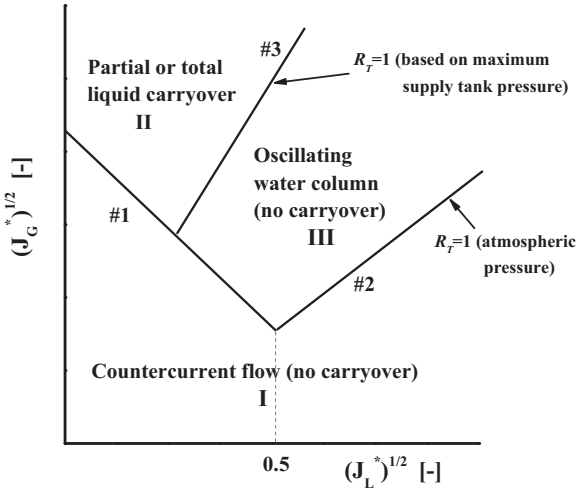

Fig. 5. Idealized flow regime map for steam–water flow in an elbow (Wan, 1986).

larger the sub-cooling temperatures, the higher the gas velocity at CCFL. This finding effect was confirmed by Chun and Yu (2000), who examined the effect of steam condensation on CCFL in nearly horizontal two-phase flow. The difference in the CCFL data between steam–water and air–water in those regimes related to the complete condensation of injected steam by sub-cooled water under the influence of a water column head in the vertical leg. To explain this behaviour, Wan defined the thermodynamic ratio R_T as

$$R_T = \frac{m_L C_p (T_{sat} - T_L)}{m_G h_{LG}} \tag{11}$$

For $R_T = 1$ (atmosphere pressure), Eq. (11) can be arranged to give

$$J_G^* = \frac{\rho_L^{1/2} C_p (T_{sat} - T_L)}{\rho_G^{1/2} h_{LG}} J_L^* \tag{12}$$

where T_{sat} and T_L are the saturation temperature and liquid temperature respectively. Cp is the specific heat of liquid at constant temperature at constant pressure, and h_{LG} is the specific enthalpy. Here flooding would be expected to take place for a steam flow only in the region above the $R_T = 1$ line.

Gardner (1988) and Tehrani et al. (1990) used the same experimental apparatus to study the flooding in a 1/9th scale model of the hot leg system of the proposed Sizewell 'B' PWR. The inner pipe diameter was 84 mm. Air and water were used as test fluids. In those works the data on the "low head flooding" and "high head flooding" that correspond respectively to the terms of "CCFL" and "deflooding" in the present review article were observed. The effects of the form of entry to hot leg at the reactor pressure vessel end and the presence of the tube bundle in the steam generator on them were also examined. The CCFL data were presented in terms of the Wallis parameters. Their studies found that at low liquid flow rate ($J_L^{*1/2} < 0.15$) the CCFL data is independent of the above effects. In comparison between flooding and deflooding experimental data shown that deflooding data are substantial the same as those for flooding only for low liquid velocities. This indicated that the hysteresis between flooding and deflooding experiments appeared.

In order to clarify the effects of the inclination angle of the lower leg on the CCFL and the physical mechanisms involved in a complex piping system, Kawaji et al. (1991) performed a flooding experiment in vertical to inclined and vertical to horizontal pipes. The inner pipe diameter was 51 mm. They found that at low to moderate liquid flow rates ($J_L^{*1/2} < 0.6$) the CCFL in vertical-to-downwardly inclined pipes are higher than that in vertical to horizontal pipes. The effect of pipe inclination was not observed in their experiments. This data is a contradictory to that of Wan and Krishnan (1986) who examined the effect of small change of lower leg inclination angle, although the experiments were conducted under the same flow conditions. Next, it is also a contradictory to the data of Barnea et al. (1986), who examined the effect of pipe inclination angle on the CCFL in inclined pipes under the same inner pipe diameter, but without elbow. The possible reason is due to the difference in the involved flooding mechanisms. In Kawaji et al. experiments, the flooding mechanisms depended on the liquid flow rate. For $J_L^{*1/2} < 0.4$, it is initiated by the slugging near the elbow, and the liquid entrainment and carryover for $J_L^{*1/2} < 0.4$. On the other hand, in Barnea et al.'s experiments, it is initiated by nature of slugging. In the present literature, Kawaji et al. also performed a semi analytical study to predict the CCFL data in their experimental configuration on the basis of the observed flooding mechanisms, and this will be discussed in Section 3.2 of the present review article.

Wongwises (1994, 1996a,b) experimentally studied CCFL in a model of the PWR hot leg with a broad range of the horizontal leg to inner diameter pipe ratios and inclination angles of the inclined riser. The inner pipe diameter was 64 mm. The test fluids were air and water. A conductance cell was implemented to measure the liquid hold-up near the bend of the horizontal leg within the uncertainty ±2%. The flow phenomena were detected by visual observations and sometimes by high-speed cameras. The CCFL data were presented in terms of Wallis parameters. Wongwises (1994, 1996a) reported that the CCFL curves can be divided into three regions, in each of which the mechanism is different. The mechanisms are dependent on the water flow rate. In first region ($J_L^{*1/2} < 0.2$), CCFL decreases as the liquid flow rate increases. The flooding appears simultaneously with the slugging of unstable waves which are formed at the crest of the hydraulic jump. The position of the hydraulic jump is dependent also on the water flow rate. At very low water flow rates, the hydraulic jump appears near the bend, and shifts away from the bend with the increase of the water flow rate. In the second region ($0.2 < J_L^{*1/2} < 0.35$), the CCFL increases as the water flow rate increases. Here the flooding locus coincides with the location of the onset of slugging in the horizontal leg accompanied by partial or total carry over of the injected water. In the third region ($J_L^{*1/2} < 0.35$), the CCFL decreases as the liquid flow rate increases. The flow is supercritical throughout the horizontal leg, and no hydraulic jump is observed.

Next, Wongwises found that the gas velocity at CCFL decreases with the increase of the length of horizontal leg. The inclination angle of the riser and the water inlet method play an important role on flooding in the range of intermediate and high liquid flow rate. Moreover, the void fraction near the bend around the CCFL, in which the flooding coincides with the onset of slugging near the bend, was proposed as follows.

$$J_G^* = 0.82 \alpha_G^{2.75} \tag{13}$$

Similar flooding mechanisms as described in the previous paragraph were also reported by Geweke et al. (1992), Kang et al. (1999), and Chun et al. (1999) under the difference of scale model of PWR hot leg. Last two literatures from the same groups in Korea reported the CCFL in a model of the PWR hot leg of the Korean standard nuclear power plant (KNSPP, Ulchin 3 and 4). Finally, Kang et al. proposed an empirical correlation in terms of Wallis parameters to predict the initiation of flooding in the first region ($J_L^{*1/2} < 0.2$) as below.

$$(J_G^*)^{1/2} + 0.397 (J_L^*)^{1/2} = 0.603 - 0.00234 \left(\frac{L_H}{D} \right) \tag{14}$$

Author's personal copy

Eq. (14) shows that the inclination angle of the inclined riser does not play an important role as reported Kawaji et al. It is also contradictory to that reported by Wongwises. However there were no available explanations on it.

Later Eq. (14) was corrected by Kim and No (2002), which assessed a total of 356 experimental CCFL data through a literature survey from 1986 to 1996, and is written as follow.

$$(J_G^*)^{1/2} + 0.614(J_L^*)^{1/2} = 0.635 - 0.00254\left(\frac{L_H}{D}\right) \quad (15)$$

They claimed that the proposed correlation agrees well with the literature database within the prediction error, 8.7%.

Gargallo et al. (2005) performed an experimental study regarding the occurrence of hydraulic jumps in air–water counter-current two-phase flow by using the WENKA test facility from Forschungszentrum Karlsruhe (FZK), Germany. The acronym WENKA stands in German for "Wasser und Entrainment Kanal", what means "Water and Entrainment Channel". The major objective of their work was to identify flow regimes and understand the physics of the transition from stable stratified flow to reversed flow. For this purpose a super-critical water flow was injected to a rectangular channel in counter-current to the air flow in order to simulate the injection of emergency core cooling (ECC) through the "Hutze" in the hot leg of German PWR. They found that a hydraulic jump occurs is an initiator for a water flow reversal. Finally, they used the experimental data to validate their one-dimensional model to predict the counter-current flow limitations during hot leg injection in pressurized water reactors. The model indicates that not only the nondimensional superficial velocities of liquid and gas, but also the Froude number of the liquid at the injection point and the Reynolds number of the gasplay an important role for the prediction of flow reversal.

Navarro (2005) conducted experimental studies on the CCFL in small scale geometry of the PWR hot legs. The water levels (void fractions) in three positions along the horizontal leg were measured using attenuation of gamma-radiation. Next, the effects of the geometrics of test channel on CCFL were observed. Finally, Navarro proposed a basic formula to predict the CCFL for the test models in a quadratic form of the Wallis parameters, and when it applied to the dimensions of a PWR hot leg can be written to a simpler equation as follow.

$$(J_G^*)^{1/2} = 0.5963 - 0.2452(J_L^*)^{1/2} - 1.17J_L^* \quad (16)$$

Experiments focusing on the validation of the CFD codes on CCFL in a model of PWR hot leg are rather limited. The serial works of the groups from *Helmholtz-Zentrum Dresden-Rossendorf* (HZDR) in Dresden (Germany), and Tomiyama and his coworkers in Kobe (Japan) are exceptions to this, and will be described in the next sections.

For the sake of the CFD code validation, it is more important to ensure a good access for measurements of distributed flow parameters than to create an exact geometrical similarity with the original. In many facilities where CCFL experiments were carried out previously, optical access was possible (e.g. acrylic glass test section, sight glass). The observation of the flow was mainly used to support the interpretation of the results. The few pictures of the flow published in the past from experiments in hot leg typical geometries do not allow the recognition of detailed structures like bubbles and droplets. Furthermore, since these investigations were performed in pipes, the optical quality was limited by the 3D shape of the interfacial structure. For those reasons, CCFL experiments using advanced experimental technologies in a rectangular channel of a model of PWR hot leg were carried out by Deendarlianto et al. (2008), Vallée et al. (2008, 2009), and Lucas et al. (2008) from the research groups of HZDR.

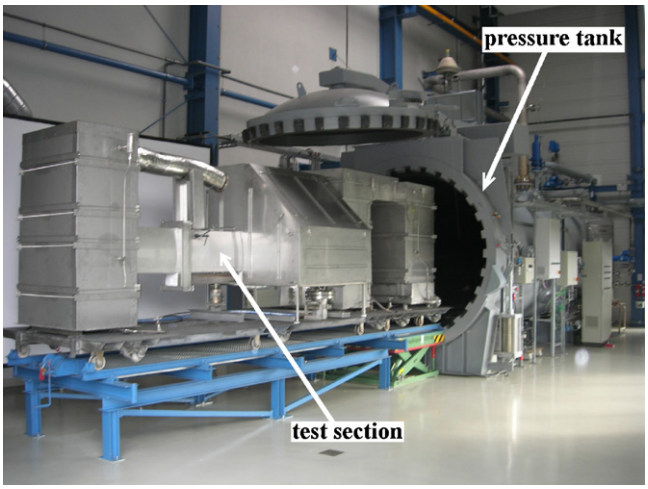

Fig. 6. Pressure vessel of the TOPFLOW facility (Deendarlianto et al., 2008).

In their studies, the cross section of rectangular channel was of 0.05 m × 0.25 m. The height of the rectangular test section (0.25 m) represented the inner pipe diameter of hot leg pipe of a PWR from the German *Konvoi* type at a scale of 1:3. The combinations of test fluids were air–water (Deendarlianto et al. and Vallée et al.) and steam–water (Lucas et al.). The test section was put in a pressure chamber, in which it was operated in pressure equilibrium with the inner atmosphere of the tank in TOPFLOW (transient two-phase flow) facility as shown in Fig. 6. In their works, the detail flow behaviour in the bended region during a series of flooding and deflooding experiments was captured by a high-speed camera. Similar flooding mechanisms as reported by the previous investigators (Wongwises et al., Kang et al., and Chun et al.) using circular pipes were obtained. The flooding mechanisms were not influenced by the changing of system pressures (Deendarlianto et al. and Vallée et al.), and the combination of test fluids (Lucas et al.). Next, the Wallis-parameter $J_K^{*1/2}$ can be applied to rectangular cross-sections by using the channel height as a characteristic length instead of the inner pipe diameter. The CCFL data of air–water test were in agreement with the available experimental correlations obtained from circular pipes in the range of low liquid flow rate ($(J_L^*)^{1/2} < 0.12$). Moreover, a hysteresis between the flooding and deflooding experiments was investigated, and increases with the increase of water flow rates (Deendarlianto et al., 2008).

Tomiyama and his co-workers from *Kobe-Japan* performed a series experimental works to establish the experimental database for improvement and validation of numerical analysis models as shown in the papers of Minami et al. (2008a, 2010a) and Nariai et al. (2010). The test fluids were air and water. In their works, the test sections were rectangular channel (Minami et al., 2008a) and circular tube (Minami et al., 2010a; Nariai et al., 2010). In the case of rectangular test channel, the cross section was 150 mm × 10 mm. The height of this rectangular cross section represented 1/5th of the diameter of the PWR hot leg. For this test channel, the flow patterns along the channels and CCFL characteristics were investigated. The water levels along the horizontal and inclined legs were measured by using resistance method of parallel wire probes. The CCFL data were presented in terms of the phases Wallis-parameter, J_K^*, whereas the hydraulic diameter was used as a characteristic length. They found that the flow patterns in the elbow and inclined sections were strongly affected by those in the horizontal sections. The CCFL data are consistent with the Wallis-type correlation and a linear relationship between $J_L^{*1/2}$ and $J_G^{*1/2}$ was found. Moreover the void fractions along the pipe under CCFL condition were also correlated as tabulated in Table 2.

Author's personal copy

Table 2
Void fraction around the CCFL along the rectangular cross section (Minami et al., 2008a).

Locations	Void fraction under CCFL
Horizontal channel near elbow	$\alpha_G = 0.245 + 0.419J_G^*$
End of horizontal channel near RPV	$\alpha_G = 0.665 + 0.38J_G^*$
Inclined section	$\alpha_G = 0.70(J_G^*)^{0.3}$

To investigate the CCFL in a small-scale PWR hot leg Minami et al. (2010a) also carried out experimental works in a circular pipe. The inner pipe diameter was 50 mm, represented a 1/15th scale down of inner pipe diameter of PWR hot leg. The test fluids were also air and water. The conclusions of this work were almost similar to those of in rectangular cross sections. In addition, the CCFL characteristics obtained by increasing $J_G^{*1/2}$ differed from those obtained by decreasing $J_G^{*1/2}$. This means that a hysteresis between flooding and deflooding appeared.

Recently in cooperation with the experimental group of HZDR, Nariai et al. (2010) from the group of Tomiyama examined also the effect of the fluid properties on CCFL by using water and glycerol–water solutions for the liquid phase. They found that the surface tension and liquid viscosities showed a little effect on the CCFL. This is in contrast to the result of Zapke and Kroger (2000) for straight vertical tubes and illustrates the effect of test section geometry.

3.1.2. Multiple elbows

Table 3 shows the summary of the experimental studies on the countercurrent flow in a model of PWR hot leg using multiple elbows. Compared with the similar study of the counter-current flow in a complex piping system using a single elbow, the similar study using multiple elbows is rather rare.

The earliest research work was performed by Krolewski (1980). She carried out experimental works to study the flooding and deflooding in a complex piping system using double elbows. The test fluids were air and water at atmospheric conditions. The test facility consisted of a 51 mm inner pipe diameter, 584 mm long horizontal leg connected to vertical and inclined pipes by either a 90° or a 45° from horizontal. Since not all reactors have the same primary loop geometry, five different pipe configurations are tested. Her experimental results indicated that the geometry of the hot leg pipe has a significant effect on the CCFL. Change in flooding location caused a slight change in the slope of CCFL curve. Hysteresis was significant only in configurations which had 45° elbows at one end of the test sections. For the flow rates with the highest hysteresis effect, the water flow was subcritical at the higher limit and supercritical at the lower limit. The change from subcritical to supercritical flow may account for the wide range of hysteresis.

Kawaji et al. (1993) carried out flooding experiments in adiabatic air/water system for three piping geometries each containing three elbows and an orifice in order to understand the physical mechanisms involved. The inner pipe diameter was 51 mm. The tested piping systems were double-vertical elbow, double-horizontal elbow, and double-inclined elbow. The CCFL was detected by visual observation. The CCFL data was presented in terms of Wallis parameters. They reported that the vertical-to-horizontal geometry with multiple horizontal sections connected by 90° elbows result the lowest CCFL data. Inclining one of the horizontal sections downward eliminated the hydraulic-jump-induced flooding mechanism in that section and increased the CCFL. Next, the placement of an orifice decreased the CFFL. The last conclusion has been accepted by Tye (1998) who studied the effect of obstructions on CCFL in vertical and horizontal tubes.

Table 3
Summary of investigations on the counter-current flow study in a model of PWR hot leg using multiple elbows.

Researcher/year	Experimental conditions	Practical analogy	Analytical study	Experimental Study	Remarks
Krolewski (1980)	– Air–water test – Circular tube Different angles, inner diameter & configurations (see attachment)		N/A	Configuration and hysteresis effects on CCFL	– The geometry of the hot leg has a significant effect on the flooding limit – Hysteresis was significant only in configuration of elbow inclination angle $\beta = 45°$. The change from subcritical to supercritical flow may account for wide range of hysteresis – Change in flooding location cause a slight change in the slope of flooding curve. Flooding limit for each pipe fitting is probably slightly different
Kawaji et al. (1993)	– Air–water test – Circular tube of inner diameter = 51 mm –Tested pipe configurations 1. Double-vertical elbow 2. Double-horizontal elbow 3. Double inclined elbow	Model of CANDU PWR hot leg	**Semi-analytical studies**	Configuration effects on CCFL and involved mechanisms	– New method based on the superposition principle was proposed to predict the flooding condition for complex piping systems – The effects of the inclining one of the horizontal sections downward on CCFL and involved mechanisms were clarified from experiment
Noel et al. (1994)	– Air–water test – Circular tube of inner diameter = 3/4 in. – Two types of complex piping system (see Fig. 7)	1:4 scale down model of CANDU PWR hot leg	N/A	Configuration and hysteresis effects on CCFL	– Empirical CCFL correlations of the represented test piping system were proposed. – Superposition principle proposed by Kawaji et al. (1993) was not able to predict CCFL.

Author's personal copy

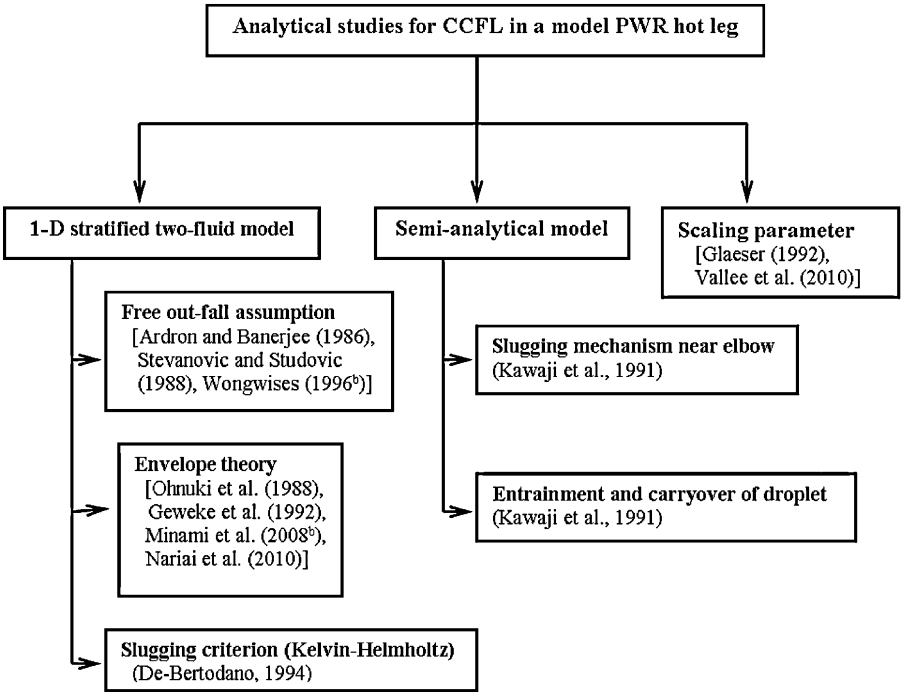

Fig. 7. Classification of analytical models on the countercurrent flow in a model PWR hot leg.

In relation to the configuration of the PWR hot leg of the CANDU reactors, Noel et al. (1994) performed an air–water flooding experiment. Two test sections were used. The first test section was essentially a 1/4 scale down model representing the complexity of CANDU feeders. It included ten elbows, four vertical sections, five horizontal sections, and five inclined sections. It referred to as the "0° inclined test section". The second was basically the same construction to the first one except that all the horizontal sections had a 5° downward inclination. The inner pipe diameter of both test section was 19 mm. In their studies, the CCFL and hysteresis between flooding and deflooding experiments were clarified. They found that the declining of the horizontal sections shifted the CCFL curves upward. Hysteresis between flooding and deflooding occurred only in the 5° inclined test section (second test section). Based on their experimental data, the empirical correlation to predict the flooding and deflooding point in their geometries were proposed as follows.

For the 0° inclined test section:

$$(J_G^*)^{1/2} = [0.139 - 0.827 J_L^*]^{1/2} \quad \text{(Flooding \& deflooding)} \tag{17}$$

For the 5° inclined test section:

$$(J_G^*)^{1/2} = 1.675 - 9.50(J_L^*)^{1/2} + 25.77 J_L^* - 25.52(J_L^*)^{3/2} \quad \text{(Flooding)} \tag{18}$$

$$(J_G^*)^{1/2} = -0.455 - 10.21(J_L^*)^{1/2} - 32.64 J_L^* + 28.05(J_L^*)^{3/2} \quad \text{(Deflooding)} \tag{19}$$

In addition, a strong cyclic flooding phenomenon as proven in the data of time wise of pressure drop was observed for the air injection below $J_G^* \approx 0.33$. However the scientific reason for this effect was not discussed.

3.2. Analytical studies

To explore the dynamics around the CCFL in a PWR hot leg, analytical models are needed. Several types of analytical studies have been carried out, focussing on the prediction of the gas velocity at the inception of flooding, and the assessment of the proposed analytical models to real size of PWR hot leg. The available analytical studies are broken down into three categories. Those are (1) one-dimensional stratified two-fluid model, (2) semi-analytical studies, and (3) scaling parameters. Those are classified in Fig. 7, and described respectively in the following.

3.2.1. One-dimensional stratified two-fluid model

To determine the CCFL in a PWR hot leg, 1D stratified two-fluid model was considered to be used. To solve the momentum and mass conservation equations in this model, three different viewpoints on the basis of flooding mechanisms were proposed in the literature. The first group considers that the flooding coincides to the slugging inception in the lower leg of the elbow close to the bend. Meanwhile the second group suggests use of the envelope theory to solve the momentum balance equation between the two-phase in the horizontal part of the model of PWR hot leg. The last view point implements the available slugging criteria to solve the momentum balance equations in this model. In any case a purely theoretical approach seems to be very difficult, whereas most of researchers used simplified equations from experiments for countercurrent flow parameters.

The first group was initiated by Ardron and Banerjee (1986). This model was developed originally on the basis of the observed flooding mechanisms of the experimental work of Siddiqui et al. The concept of this model is based on the steady state mass and momentum balance equations for a counter-current stratified flow of a liquid film and a gas in a horizontal pipe. CCFL is assumed due to the onset of slugging in the lower leg of the elbow close to the bend, where the liquid depth is greatest. The liquid level from the hydraulic jump to the horizontal leg outlet decreases continually. A free out-fall is assumed at the horizontal leg exit, implying that the liquid velocity at this point is equal to critical velocity (the gradient of the gas void fraction is infinitive). Here viscous interactions and pressure changes at the interface caused by surface tension are neglected. Assuming turbulent gas and liquid flow, finally they

Author's personal copy

obtained the critical velocity at the horizontal leg exit, when α_G satisfies the below equation

$$\frac{\pi\alpha_L\alpha_G}{4\tilde{S}_i} - \frac{\alpha_L}{\alpha_G^2}(J_G^*)^2 - \frac{\alpha_G}{\alpha_L^2}(J_L^*)^2 = 0 \tag{20}$$

where $\tilde{S}_i$ is the normalized of the width of the gas–liquid interface.

Eq. (20) relates to the void fraction at the horizontal leg exit to J_L^{*2} and J_G^{*2} just before flooding inception. To obtain the relationship between those Wallis parameters' in terms of L_H/D and the physical properties, Eq. (20) should be solved together with the momentum equations of each phase. Here, an iterative procedure coupled with purely empirical correlations should be used in order to obtain the solution. Those empirical correlations include the void fraction at the locus of the hydraulic jump near the pipe bend (α_G), phase-wall friction factors (f_{wk}), and interfacial shear stress (τ_i) as tabulated in Table 4. From this study, Ardron and Banerjee obtained also a CCFL curve in the vertical-to-horizontal elbow by using the quadratic fit for $0 \le J_L^* \le 0.9$ as

$$J_G^{*1/2} = 0.447 - 0.176J_L^{*1/2} - 0.263J_L^* \tag{21}$$

In Eq. (21) the flow was assumed as an "ideal frictionless flow", whereas the gas void fraction near the elbow is equal to that of the horizontal leg exit. It should be noted that the interfacial friction has a significant effect on flooding. Therefore the ideal friction flow assumption is not true physically. This means that Eq. (21) appears to be an alternative method rather than a new equation for predicting CCFL in a model of PWR hot leg.

The second group applied the envelope theory to solve the momentum equations in the two-fluid model. Models based on this approach include the work of Ohnuki et al. (1988), Geweke et al. (1992), Minami et al. (2008b), and Nariai et al. (2010). The assumptions of uniform flow in steady state, no entrainment, and no phase change were taken. The envelope is employed to the locus of tangents to the operating lines in the (J_G^*, J_L^*) plane for a constant void fraction and thus represents a limiting curve separating the operating region from an unattainable region for countercurrent flow (Bankoff and Lee, 1985). In this group, it is considered also that the CCFL corresponds to the retardation of the liquid film due to the interfacial shear stress. Therefore, three friction coefficients also play an important role in the calculation. They are available in literatures, and summarized in Table 5.

The last group implemented the onset of slug flow criteria as a flooding criterion in a model of the PWR hot leg. Here the flooding point is determined by the integration of the momentum equations of a one-dimensional two-fluid model, whereas this slug criterion was used as a boundary value. This method was introduced by De Bertodano (1994). The important parameters in this approach are three friction factors and momentum loss of the elbow. In this calculation, De Bertodano assumed that $f_{wk} = 0.04$ and $f_i = 2f_L$. The hydraulic losses at the elbow were modelled by extending the length in the horizontal section. Based on this approach, De Bertodano showed that the hydraulic jump observed in the small scale experiment of Krolewski does not occur in a full scale PWR hot leg. Finally De Bertodano recommended a general flooding correlation in a PWR hot leg as

$$J_{GL}^{*1/2} + 0.676J_L^{*1/2} - 1.019e^{-61.75J_L^{*1/2}} = 0.640 \tag{22}$$

Eq. (22) was obtained for the countercurrent steam–water two-phase flow at 0.3 and 1.5 MPa. This equation is difficult to use because an additional expression is needed to calculate the gas void fraction in order to obtain the dimensionless relative velocity of gas and liquid (J_{GL}^*). Derived from a fit of this equation, De Bertodano proposed a CCFL correlation under full scale conditions of PWR hot leg as

$$J_G^{*1/2} + 0.798J_L^{*1/2} = 0.619 \tag{23}$$

3.2.2. Semi analytical model

From the visual observation, Kawaji et al. (1991) developed two semi-analytical methods to determine the CCFL in this complex piping system. Those are slugging mechanism near the elbow and entrainment of liquid droplet. In those methods, the relative velocity between the gas and liquid near the elbow at the flooding inception must be accurately determined. It was taken from the assumption that the annular flow in the vertical pipe is maintained for some distance past the elbow in the entrance section of the inclined leg. The gas void fraction near the elbow can be calculated from the available liquid film thickness equation of annular flow.

For the slugging mechanism near the elbow, Kawaji et al. modified a correlation of slugging criterion near horizontal pipe proposed by Taitel and Dukler (1976). Their modified equation can be written as

$$\frac{J_G}{\alpha_G} + \frac{J_L}{\alpha_L} = \frac{0.5(\alpha_G)^{1/2}}{\sqrt{\rho_G/(\rho_L - \rho_G)\, gD\, \cos\theta}} \tag{24}$$

where θ is the inclination angle of the lower leg to the horizontal. They reported also that Eq. (24) is in agreement with their experimental data for low liquid flow rate, in which the inclination of the lower legs were 112.5° and 135° from vertical.

For the second mechanism, Kawaji et al. (1991) considered the entrainment and carryover of droplets generated as a result of the breakup of the turbulent jetlike liquid stream. The break-up is necessary but not a sufficient condition for flooding, as the droplet must be entrained and carried upstream by the gas flow. In this approach a simple force balance on a droplet of given diameter moving in a countercurrent flow of a gas with a relative velocity ($v_G + v_L$) was considered. To prevent the droplets from falling down into the liquid stream flowing along the bottom of the inclined pipe, the relative velocity must be sufficient high to balance the vertical components of drag, gravity, and buoyancy forces on a droplet of diameter D_d. Assuming that the droplet is spherical, the final equation for the minimum relative velocity required for droplet carryover can be described as

$$\frac{J_G}{\alpha_G} + \frac{J_L}{\alpha_L} = \frac{2}{\sqrt{3}}\left[\frac{g(\rho_L - \rho_G)D_d}{\rho_G C_D\ \sin\theta}\right]^{1/2} \tag{25}$$

For a given droplet diameter, Eq. (25) is solved iteratively using the available drag coefficient correlation (C_D) in the literature applicable to a spherical particle such as proposed by Wallis (1969) as

$$C_D = \begin{cases} \dfrac{24}{Re_d} & Re_d < 1 \\ \dfrac{24}{Re_d}(1 + 0.15Re_d^{0.687}) & 1 < Re_d < 10^3 \\ 0.44 & 10^3 < Re_d < 2 \times 10^5 \end{cases} \tag{26}$$

where

$$Re_d = \frac{\rho_G(v_G + v_L)D_d}{\mu_G} \tag{27}$$

They reported that this model is in agreement with their experimental data at the liquid superficial velocities greater than about 0.15 m/s when the inclinations of the lower leg were 135° and 157.5° from vertical, for which the slugging mechanism model does not apply. Here a constant Weber number based on local liquid velocity ($We = \rho_L v_L^2 D_d/\sigma$) was chosen as $We = 100$. However Tye (1998) is in disagreement with this approach. Tye noticed that the use of the liquid density and velocity in the Weber number

Author's personal copy

Table 4
Different proposed empirical correlations to solve Eq. (18) and momentum equations in 1D two-fluid model approach.

References/year	$\alpha_{G,slug}$ near the elbow [−]	f_{wk} [−]	τ_i [N/m^2]
Ardron and Banerjee (1986)	$J_G^* = 0.2\,\alpha_G{}^{3/2}$ (From Siddiqui et al., 1986)	$f_{wk} = CRe_k^{-n}$ For turbulent flow, $C = 0.046$ & $n = 0.2$ For laminar flow, $C = 16$ & $n = 1$	$\tau_i = \tau_{wG}$
Stevanovic and Studovic (1995)	$J_G^* = 0.2\,\alpha_G{}^{3/2}$ (From Siddiqui et al., 1986)	$f_{wk} = CRe_k^{-n}$ For turbulent flow, $C = 0.046$ & $n = 0.2$ For laminar flow, $C = 16$ & $n = 1$	$\tau_i = f_i \frac{\rho_G}{2} \lvert u_G - u_L \rvert (u_G - u_L)$ For the smooth liquid film, $f_i = f_{GW}$ (From Taitel and Dukler, 1976) For the wavy liquid film, $f_i = 0.14 \times 10^{-5}\mathrm{Re}_F + 0.021$ (From Kim et al., 1986)
Wongwises (1996b)	$J_G^* = 0.82\,\alpha_G{}^{2.75}$	$f_{wk} = C\,Re_k^{-n}$ For turbulent flow, $C = 0.046$ & $n = 0.2$ For laminar flow, $C = 16$ & $n = 1$	$\tau_i = \tau_{wG}$

implies that the drop size is controlled at formation. His disagreement is supported by the theory of Smits et al. (1993) and Kocamustafaogullari et al. (1994). Those theories indicated that the drop size is controlled by break-up mechanisms caused by the interaction of the droplet and the gas stream. Therefore it yields physically unrealistic droplet size at low liquid velocities.

In the case of analytical or semi-analytical works on the CCFL in a PWR hot leg using multiple elbows was limited to be found in open literatures. For this purpose, Kawaji et al. (1993) introduced "a superposition principle". In this principle the piping system is represented as a combination of simple geometries (vertical, horizontal or inclined pipes). The most limiting gas velocities as each liquid flow rate are combined to obtain the predicted CCFL conditions over the entire range of liquid flow rates. Later Noel et al. reported that this simple superposition method was not able to predict the CCFL in complex piping geometries of 1/4 scale of the feeder pipes of a CANDU reactor.

3.2.3. Scaling parameters

The determination of suitable parameters to correlate the CCFL data is one of the purposes of the researches on countercurrent gas–liquid two-phase flow. Meanwhile the experimental data to fulfil this effort are not sufficient. The development of scaling laws from the view point of analytical work is a possible solution. However, there is only one paper (Glaeser, 1992) related to the development of scaling parameter from the view point of an analytical solution.

Glaeser (1992) provided a simple theoretical basis for the extension of the flooding equation in order to decide the suitable scaling parameters between the Wallis parameter and the Kutateladze number of countercurrent flow in a full geometry reactor scale. In this work, the scaling parameter in a separated countercurrent flow in a PWR hot leg is assumed as that in a horizontal pipe. The final equation of his work (Eq. (16) of his paper) leads into Wallis parameter as written in Eq. (2) of the present article review. As a result Glaeser concluded that the Wallis parameter can be applied for the countercurrent flow in a horizontal large pipe, therefore there is no chance to the Kutateladze number criterion in contrast to vertical countercurrent flow.

In order to be able to determine the appropriate characteristic length in the Wallis parameter to correlate the CCFL in a model of PWR hot leg, Vallée et al. (in press) performed a comparison studies on the air–water CCFL data of HZDR obtained from a rectangular cross-section with similar experimental data. A detailed comparison of the rectangular cross section test facility operated at the *Kobe University* (Minami et al., 2008a) and at HZDR was done. Here, clear differences in the dimensions of the cross-section ($H \times W = 150\,\mathrm{mm} \times 10\,\mathrm{mm}$ at *Kobe University*, $250\,\mathrm{mm} \times 50\,\mathrm{mm}$ at HZDR) make it possible to point out the right characteristic length for hot leg models with rectangular cross-sections. They found that the channel height is the characteristic length to be applied to the Wallis parameter for channels with rectangular cross sections. In comparison to the CCFL data obtained at the *Kobe University*, the HZDR data was obtained at slightly higher gaseous Wallis parameters. This effect occurred due to the aspect ratio chosen for the Kobe test section is too large ($H/w = 15$), which affects the flooding behaviour.

Some additional remarks are given regarding the analytical and semi analytical studies on the countercurrent flow in a model of PWR hot leg:

1. Although all the investigator of the analytical works reported a successful analytical model development, there was no an agreement on the using of interfacial friction factor as an important parameter as shown in Tables 4 and 5. Therefore it is possible to conclude that the developed analytical models agree well only with their own data or selected data in their range of validity.
2. The user adjustment in the calculations still cannot be avoided, although some reasons were provided. For example, De Bertodano reduced the coefficient of the slug flow criterion of Mishima and Ishii from 0.487 to 0.3 to match the experimental data of Ohnuki et al. with his model. Then, the using of $We = 100$ of Kawaji et al. in their entrainment model is also another example.

Table 5
Different proposed empirical correlations implemented to momentum balance equation.

References/year	α [−]	f_{wk} [−]	τ_i [N/m^2]
Ohnuki et al. (1988)	$J_G^* = 0.5\,(\alpha_G)^{3/2}$ $(\alpha \geq 0.6)$ $J_G^* = 2.8\,(\alpha_G)^{4.8}$ $(0.5 \leq \alpha < 0.6)$	For turbulent flow, For laminar flow, $f_{wk} = 16/Re_k$	$\tau_i = f_i \frac{\rho_G}{2} \lvert u_G - u_L \rvert (u_G - u_L)$, where $f_i = 1.84 f_{wL}$
Minami et al. (2008a,b)	Near the bend, $\alpha_G = 0.245 + 0.419 J_G^*$ At horizontal leg exit, $\alpha_G = 0.665 + 0.380 J_G^*$	$f_{wk} = 0.02$	$\tau_i = f_i \frac{\rho_G}{2} \lvert u_G - u_L \rvert (u_G - u_L)$, where $f_i = 0.04$
Nariai et al. (2010)	$\alpha_G = 0.94 (J_G^*)^{0.316}$	For turbulent flow, $f_{wk} = 0.079 (Re_k)^{-0.25}$ $(Re_k \leq 10^5)$ $f_{wk} = 0.0008 + 0.05525 (Re_k)^{-0.237}$ $(Re_k > 10^5)$ For laminar flow, $f_{wk} = 16/Re_k$	$\tau_i = f_i \frac{\rho_G}{2} \lvert u_G - u_L \rvert (u_G - u_L)$, where $f_i = 0.0074$

Author's personal copy

3. The analytical or semi-analytical works of the countercurrent flow in a model of PWR hot leg using multiple elbows are not enough to understand the CCFL mechanisms. Further improvement of the superposition principle proposed by Kawaji et al. should be a promising way.

In summary of the review of the analytical studies of this topic, it is suggested that the further researches in the above aspects are encouraged in the near future.

4. Computational fluid dynamics (CFD) modelling

The detailed three-dimensional (3D) information of the transient behaviour around CCFL in a model of PWR hot leg becomes a new requirement in the reactor safety analysis. The interactions between the phases, which are determined by interfacial transfers, can only be revealed by computational fluid dynamics (CFD). CFD allows substituting geometry-dependent empirical closure relations with more physically justified closure laws that are formulated at the scale of the structures of the gas–liquid interface. In this way, CFD is more flexible than one-dimensional analytical solution, in terms of transferability of models to changes in geometrical and thermodynamic boundary conditions.

The introducing of CFD method on the countercurrent flow in a model of PWR hot leg includes the investigation of CCFL mechanisms, heat transfer effects, flow patterns, hysteresis behaviour, and the extension of the obtained flow behaviour from small scale to full reactor scale. However, the available literature regarding this important topic is rare. The serial works of Wang and Mayinger (1995) from Muenchen-Germany, Murase and his co-workers in Tsuruga-Japan, Deendarlianto and his co-workers in Dresden-Germany are exception to this. In order to identify the scientific progresses on this effort, a brief review on this subject is presented here.

Wang and Mayinger (1995) simulated a thermal-hydraulic phenomena specific in the counter-current flow under UPTF experimental conditions. The calculations were conducted for two-dimensional, steady state, adiabatic and incompressible. Here mass and momentum balances for each phase were treated separately. The interphase momentum transfer is denoted by the interfacial friction factor. For this reason, they implemented empirical correlations of the interfacial friction proposed by Lee and Bankoff (1993) and Ohnuki (1986) into the code FLOW3D. In this calculation, inlet flow parameters were set to be constant and fully developed assumption was applied to the outlet. Turbulence was modelled as an extension of single-phase flow standard k–ε model. They reported that satisfactory results were obtained, whereas, under the reflux condensation conditions, numerical computation reveals that different flow structures appeared in the region away from flooding curve and in the region near the flooding curve. Next, the calculated water level and vapour velocity agree with the UPTF measurement results.

Murase and his co-workers in Tsuruga-Japan are in disagreement with the study of Wang and Mayinger. They claimed that the effects of wall friction cannot be correctly evaluated by using two-dimensional analysis. The given boundary conditions at the inlet and outlet of the hot leg in the above work might affect the calculated flow patterns in the hot leg. For this reason they conducted 3D CFD calculations. The summaries of their CFD works will be discussed (Murase et al., 2009; Minami et al., 2009, 2010b; Kinoshita et al., 2009; Utanohara et al., 2009).

Murase et al. (2009), Minami et al. (2009, 2010b) and Utanohara et al. (2009) conducted 3D CFD simulations on countercurrent flow in a PWR hot-leg air–water two-phase flow in a 1/15th scale model. This calculation model reproduced the size of experimental test facility at Kobe University as reported by Minami et al. (2010a). Their works included the effects of interfacial friction correlation (Utanohara et al.), flow patterns and CCFL (Murase et al., 2009; Minami et al., 2009, 2010b). They implemented the volume of fluid (VOF) and Euler-Euler two-fluid models on the commercial CFD code FLUENT6.3.26. The required interfacial friction correlations in the Euler-Euler two-fluid model were selected from a combination of available 1D experimental correlations for the cases of annular and slug flow that gave the best agreement with the experimental data. For all their calculations the total number of meshes is about 70,000. They concluded that it is better to use the two-fluid model with suitable interface friction correlation than VOF model. The predicted flow patterns, hysteresis behaviours, and CCFL characteristics agree well with their experimental data.

Kinoshita et al. (2009) carried out numerical simulation for countercurrent steam–water flow under PWR plant condition by using the same CFD code. Although the model was enlarged to be 15 times of the previous calculation model, the number of meshes was similar. In comparison to their previous works it is noticed that the interfacial friction correlation used in this calculation is still the same. In the analysis of the plant condition, they showed that the hysteresis appeared in the increasing and decreasing stages of steam flow rates. It has a contradictory to their original assumption that the waves were likely to develop so hysteresis did not appear. This is possible due to their calculation meshes being relatively large, which is not recommended by the best practice guidelines (BPG) for the use of CFD in nuclear reactor safety applications (Menter, 2002). In this BPG it is clearly noticed that repeat runs with different meshes should be performed to give an indication of the degree of precision of the results. In addition, the approximation of physical processes by implementation of empirical correlations in their CFD simulations might also lead to an error.

The development of a general model closer to physics and including less empiricism is a long-term objective of the activities of the HZDR research programs. Such models are an essential precondition for the application of CFD codes to the modelling of flow related phenomena in nuclear facilities. Here local geometry independent models for mass, momentum, heat transfer, and scalar transport are developed and validated. One of the developed scientific method to solve the above problems was the new concept of drag coefficient in the algebraic interfacial area density model (AIAD) (Höhne, 2009).

The AIAD model reflects the morphologies of the phases by appropriate parameters in the drag force. The ideas of the model are:

- The interfacial area density allows the detection of the morphological form and the corresponding switching of each correlation from one object pair to another.
- It provides a law for the interfacial area density and the drag coefficient for full range of void fraction. The interfacial area density in the intermediate range is set to the interfacial area density for free surface.
- The model improves the physical modelling in the asymptotic limits of bubbly and droplet flows, and the interfacial area density in the intermediate range is set to the interfacial area density for free surface.

More recently, Deendarlianto et al. (2010) from the same group of Höhne at HZDR carried a CFD simulation of the counter-current flow under HZDR experimental conditions. One air–water and one steam–water CCFL experiments were selected from HZDR test series for the CFD simulation. The simulations were carried out using a commercial CFD code of ANSYS CFX with a 3D two-fluid Euler-Euler model. In the calculation model, the grid consists of 248,610 hexahedral elements and 281,076 nodes. Due to the

Author's personal copy

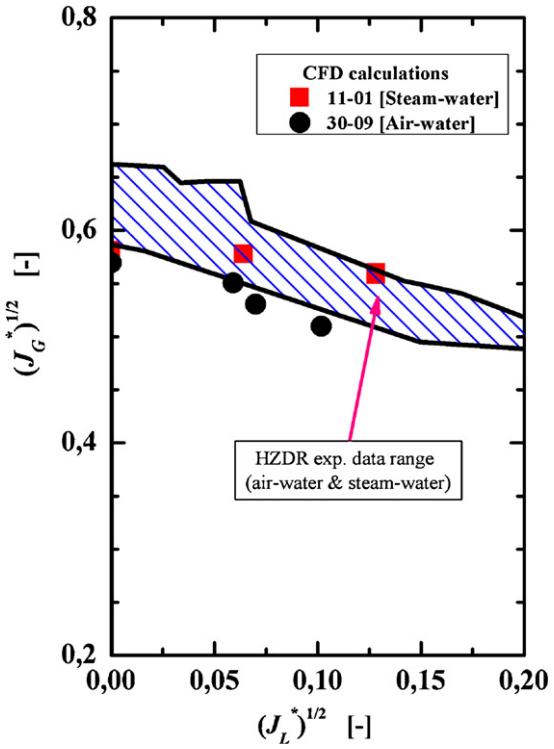

Fig. 8. Calculated CCFL characteristics in a model of PWR hot leg (Deendarlianto et al., 2010).

insufficient computer resources, grid independence test was not performed. On the other hand, very carefully developed structured mesh for most of the flow field was adequate, at which the local refinement on them were carried out. The calculations were carried out in fully transient manner using a gas/liquid inhomogeneous multiphase flow model coupled with a shear stress transport (SST) turbulence model. The time step and simulation time for each case were 10^{-4} s and four months by using four parallel processors respectively. In the simulation, the drag coefficient was approached by the AIAD model. The results indicated that quantitative agreement of the CCFL characteristics between the calculation and experimental data was obtained as shown in Fig. 8. Next the flow characteristics shown in the experiment such as the occurrence of hydraulic jump near the bended region of the PWR hot leg and liquid slug were reproduced in simulation, whereas were not possible produced using the default model of the available CFD models.

The above result (Deendarlianto et al., 2010) indicates that the AIAD model is a promising way to simulate the phenomena around CCFL in a PWR hot leg. Moreover the further improvement of the model should be carried out. Here the usage of the morphology detection algorithm should also be possible also in vertical flow regimes. Therefore it is necessary to include the modelling of non-drag forces (lift force, wall lubrication force, virtual mass force etc.) in the AIAD model as well as the available complete for polydispersed flows. Next the turbulence damping procedures should include the existence of small surface instabilities in the macroscopic model. In addition the numerical approach of the AIAD model should be improved to further reduce the calculation time.

5. Discussion

As described in the previous sections implicitly, a lot of experimental and analytical works as well as CFD modelling on countercurrent flow in a model of PWR hot leg have been performed. In spite of this, the physical mechanisms leading CCFL are still not yet fully understood, and continuously experimental efforts are still required. From the comprehensive overview of the experimental works, we can see some contradictory conclusions about flooding mechanisms, although they were carried out under the same experimental conditions. Even though, the basic topology of the hydraulic jump is not well understood, although the hydraulic jump enhances the slug formation as one of the responsible mechanism.

CCFL in a real PWR condition is a problem involving an interconnection of fluid dynamic, thermodynamic and heat transfer. Therefore it is very difficult to obtain a general conclusion from a simple experimental result in isolated condition. In other words, presently we have no physical measure to capture the important parameters on CCFL. This is undoubtedly one of the reasons why we have limited success in mechanistic modelling of flooding. For example, if we change the test liquid temperature, the physical properties of the liquid also change which accordingly affects the interfacial heat transfer between gas and liquid. However a systematically explanation regarding this point is not available in open literature. Therefore, it is very useful to investigate the effect of mass transfer on CCFL in space and time. Consequently the CCFL data of steam–water close to the real PWR model should be obtained. A wide range of system pressures and working fluid temperatures should be considered also in this experimental program in order to explore the scaling effect.

In respect to the above problem, the qualitative method to determine the effect of steam condensation on the flooding mechanisms, and local parameters should be observed. Hence, the use of advance experimental procedure and apparatus, such as the optimized optical technique and recently developed mesh wire sensor are needed in the near future. Mesh wire sensor can be used to provide the information of the cross sectional distribution of the steam volume fraction. In addition, the measurement of local temperature is also important to provide the information of the condensed steam locally. Further understandings of these components are needed to understanding of flooding mechanism and development of analytical model. In actual fact, in recent years, a lot of experimental works reported visual observations obtained using a high speed video camera. Meanwhile it was mainly used to support the interpretation of the results only, and was not possible to recognize detailed structures of flows.

The last decade has seen an increasing use of 3D CFD codes to explain the phenomena around CCFL since it cannot be predicted by traditional one-dimensional system codes with the required accuracy and spatial resolution. CFD codes contain models for simulating turbulence, heat transfer, multiphase flows, and chemical reactions. Such models must be validated before they can be used with sufficient confidence. The necessary validation is performed by comparing model results against measured data. However, in order to obtain a reliable model assessment, CFD simulations for validation purposes must satisfy strict quality criteria given in the Best Practice Guidelines (BPGs).

6. Conclusions

In the present paper, a comprehensive review on countercurrent gas–liquid two-phase flow in a PWR hot leg was presented. Experimental as well as theoretical studies on CCFL in a PWR hot leg have been critically assessed. A brief review regarding the implementation of CFD codes in this topic was also provided. The review improves our understanding on the present status of this research. Several research directions in this field have been also identified. In the long term, both experimental and analytical research efforts should be attempted in order to develop a fundamental CCFL model on the basis of systematic experimental data.

Author's personal copy

New flow measurement techniques with advance image processing should be employed to elucidate the involved mechanism around CCFL in a model PWR hot leg. The obtained experimental data using these advanced techniques will provide high reliability information in terms of space and time. Those are very useful for the validation of the analytical model development including CFD and understanding the underlying flooding mechanisms.

Acknowledgements

This work is carried out within the frame work of a current research project funded by the German Federal Ministry of Economics and Technology, project number 150 1329. The authors would like to thank Mr. Adhika Widyaparaga, mechanical engineering of Kyushu University, Japan for the discussion of the manuscript.

Deendarlianto acknowledges the *Alexander von Humboldt* (AvH) Foundation in Germany for the financial support by a postdoctoral research fellow grant in the Institute of Safety Research, Helmholtz-Zentrum Dresden-Rossendorf (HZDR) e.V., Dresden-Germany.

References

Ardron, K.H., Banerjee, S., 1986. Flooding in an elbow between a vertical and a horizontal or near horizontal pipe. Part I. Theory. International Journal of Multiphase Flow 12, 543–558.

Alekseev, V.P., Poberezkin, A.E., Gerasimov, P.V., 1972. Determination of flooding rates in regular packings. Heat Transfer Soviet Research (4), 159–163.

Bankoff, S.G., Lee, S.C., 1985. A brief review of countercurrent flooding models applicable to PWR geometries. Nuclear Safety 26 (2), 139–152.

Bankoff, S.G., Lee, S.C., 1986. A critical review of the flooding literature. Multiphase Science and Technology 2, 95–180.

Barnea, D., Ben Yoseph, N., Taitel, Y., 1986. Flooding in inclined pipe: effect of entrance section. The Canadian Journal of Chemical Engineering 64 (2), 177–184.

Celata, G.P., Cumo, N., Farello, G.E., Setaro, T., 1989. The influence of flow obstructions on the flooding phenomenon in vertical channels. International Journal of Multiphase Flow 15 (2), 227–239.

Chun, M.H., No, H.C., Kang, S.K., Chu, I.C., 1999. Countercurrent flow limitation in a horizontal pipe connected to an inclined riser. Transactions of the American Nuclear Society 81, 340–341.

Chun, M.Y., Yu, S.O., 2000. Effect of steam condensation on countercurrent flow limiting in nearly horizontal two-phase flow. Nuclear Engineering and Design 196 (2), 201–217.

De Bertodano, M.L., 1994. Countercurrent gas–liquid flow in a pressurized water reactor hot leg. Nuclear Science and Engineering 117, 126–133.

Deendarlianto, Vallée, C., Lucas, D., Beyer, M., Pietruske, H., Carl, H., 2008. Experimental study on the air/water counter-current flow limitation in a model of the hot leg of a pressurized water reactor. Nuclear Engineering and Design 238 (12), 3389–3402.

Deendarlianto, Höhne, T., Lucas, D., Vallée, C., 2010. Numerical simulation of air–water counter-current two-phase flow in a model of the hot-leg of a pressurized water reactor (PWR). In: Proceeding of the 7th International Conference of the Multiphase Flow, ICMF 2010, Tampa, FL, USA.

Gardner, G.C., 1988. Countercurrent Flooding of PWR Hot Leg, Central Electricity Generating Board Research Report No. RD/L/3358/R88.

Gargallo, M., Schulenberg, T., Meyer, L., Laurien, E., 2005. Counter-current flow limitations during hot leg injection in pressurized water reactors. Nuclear Engineering and Design 23 (5/7), 785–804.

Geffraye, G., Bazin, P., Pichon, P., Bengaouer, A., 1995. CCFL in hot legs and steam generators and its prediction with the CATHARE code. In: Proceeding of the 7th International Meeting on Nuclear Reactor Thermal Hydraulics NURETH-7, New York, USA, pp. 815–826.

Geweke, M., Beckmann, H., Mewes, D.,1992. Experimental studies of two-phase flow. In: Proceeding of European Two-Phase Flow Group Meeting. Stockholm, June, Paper No. J1.

Glaeser, H., 1992. Downcomer and tie plate countercurrent flow in the upper plenum test facility (UPTF). Nuclear Engineering and Design 133, 259–283.

Glaeser, H., Karwat, H., 1993. The contribution of UPTF experiments to resolve some scale-up uncertainties in countercurrent two phase flow. Nuclear Engineering and Design 145, 63–84.

Höhne, T., 2009. Experiments and numerical simulations of horizontal two-phase flow regimes. In: Proceeding of the Seventh International Conference on CFD in the Minerals and Process Industries, Melbourne, Australia.

Kang, S.K., Chu, I.C., No, H.C., Chun, M.H., 1999. Air–water countercurrent flow limitation in a horizontal pipe connected to an inclined riser. Journal of the Korean Nuclear Society 31 (6), 548–560.

Kawaji, M., Thomson, L.A., Krishnan, V.S., 1989. Countercurrent flooding in an elbow between a vertical pipe and a downwardly inclined pipe. In: Proceeding of the 4th International Topical Meeting on Nuclear Reactor Thermal-Hydraulics (NURETH-4), Karlsruhe, Federal Republic of Germany, pp. 20–27.

Kawaji, M., Thomson, L.A., Krishnan, V.S., 1991. Countercurrent flooding in vertical to inclined pipes. Experimental Heat Transfer 4, 95–110.

Kawaji, M., Lotocki, P.A., Krishnan, V.S., 1993. Countercurrent flooding in pipes containing multiple elbows and an orifice. JSME International Journal Series B (36), 397–403.

Kim, H.T., No, H.C., 2002. Assessment of RELAP5/MOD3.2.2γ against flooding database in horizontal-to-inclined pipes. Annals of Nuclear Energy 29, 835–850.

Kinoshita, I., Utanohara, Y., Murase, M., Minami, N., Tomiyama, A., 2009. Numerical calculations on countercurrent gas–liquid flow in a PWR hot leg (2) steam–water flow under PWR plant conditions. In: Proceeding of the 13th International Topical Meeting on Nuclear Reactor Thermal Hydraulics (NURETH-13), Kanazawa City, Japan, September 2009.

Kocamustafaogullari, G., Smits, S.R., Razi, J., 1994. Maximum and mean droplet sizes in annular two-phase flow. International Journal of Heat and Mass Transfer 37 (6), 955–965.

Krishnan, V.S., 1987. Two-phase countercurrent flow in upright pipe elbows. In: Proceeding of the International Seminar on Transient Phenomena in Two-Phase Flow, Dubrovnik, Yugoslavia, pp. 555–575.

Krolewski, S.M., 1980. Flooding Limits in a Simulated Nuclear Reactor Hot Leg. B.Sc. Thesis of MIT, August 1980.

Lee, S.C., Bankoff, S.G., 1993. Stability of steam water countercurrent flow in an inclined channel: flooding. Journal of Heat Transfer 105, 713–718.

Levy, S., 1999. Two-phase Flow in Complex Systems. John Wiley & Sons, New York, USA.

Lucas, D., Vallée, C., Beyer, M., Prasser, H.M., Deendarlianto, 2008. Experiments on the counter-current flow limitation (CCFL) in a model of a pressurized water reactor hot leg. In: Proceeding of the 5th International Conference on Transport Phenomena in Multiphase Systems, vol. 1, Bialystok, Poland, pp. 325–332.

Mayinger, F., Weiss, P., Wolfert, K., 1993. Two-phase flow phenomena in full-scale reactor geometry. Nuclear Engineering and Design 145, 47–61.

Menter, F., 2002. CFD Best Practice Guidelines for CFD Code Validation for Reactor Safety Applications. ECORA FIKS-CT-2001-00154.

Minami, N., Nishiwaki, D., Kataoka, H., Tomiyama, A., Hosokawa, S., Murase, M., 2008a. Countercurrent gas–liquid flow in a rectangular channel simulating a PWR hot leg (1): flow pattern and CCFL characteristics. Japanese Journal of Multiphase Flow 22 (4), 403–412 (In Japanese).

Minami, N., Murase, M., Nishiwaki, D., Tomiyama, A., 2008b. Countercurrent gas–liquid flow in a rectangular channel simulating a PWR hot leg (2): analytical evaluation of counter-current flow limitation. Japanese Journal of Multiphase Flow 22 (4), 413–422 (in Japanese).

Minami, N., Utanohara, Y., Kinoshita, I., Murase, M., Tomiyama, A., 2009. Numerical calculations on countercurrent gas–liquid flow in a PWR hot leg (1) air–water flow in a 1/15-scale model. In: Proceeding of the 13th International Topical Meeting on Nuclear Reactor Thermal Hydraulics (NURETH-13), Kanazawa City, Japan, September 2009.

Minami, N., Nishiwaki, Nariai, T.D., Tomiyama, A., Murase, M., 2010a. Countercurrent gas–liquid flow in a PWR hot leg under reflux cooling (I) air–water tests for 1/15-scale model of a PWR hot leg. Journal of Nuclear Science and Technology 47 (2), 142–148.

Minami, N., Murase, M., Tomiyama, A., 2010b. Countercurrent gas–liquid flow in a PWR hot leg under reflux cooling (II) numerical simulation of 1/15-scale air–water tests. Journal of Nuclear Science and Technology 47 (2), 149–155.

Murase, M., Utanohara, Y., Kinoshita, I., Minami, N., Tomiyama, A., 2009. Numerical calculations on countercurrent air–water flow in small-scale models of a PWR hot leg using a VOF model. In: Proceeding of the 17th International Conference on Nuclear Engineering (ICONE 17), Brussels, Belgium, July 2009.

Nariai, T., Tomiyama, A., Vallee, C., Lucas, D., Murase, M., 2010. Countercurrent flow limitation in a scale-down model of a PWR hot leg. In: Proceeding of the 8th International Topical meeting on Nuclear Thermal-Hydraulics, Operation and Safety (NUTHOS-8), Shanghai, China, October 2010.

Navarro, M.A., 2005. Study of countercurrent flow limitation in a horizontal pipe connected to an inclined one. Nuclear Engineering and Design 235, 1139–1148.

Noel, D.G., Shoukri, M., Abdul-Razzak, A., 1994. Two-phase counter-current flow limitations in complex piping systems. In: Proceeding of 15th Annual Conference of Canadian Nuclear Society, Montreal, Cananda, June.

Ohnuki, A., 1986. Experimental study of counter-current two-phase flow in horizontal tube connected to inclined riser. Journal of Nuclear Science and Technology 23 (3), 219–232.

Ohnuki, A., Adachi, H., Murao, Y., 1988. Scale effects on countercurrent gas–liquid flow in a horizontal tube connected to an inclined riser. Nuclear Engineering and Design 107, 283–294.

Ohnuki, A., Akimoto, H., Murao, Y., 1992. Development of interfacial friction model for two-fluid model code against countercurrent gas–liquid flow limitation in PWR hot leg. Journal of Nuclear Science & Technology 29 (3), 223–232.

Pushkina, O.L., Sorokin, Y.L., 1969. breakdown of liquid film motion in vertical tubes. Heat Transfer Soviet Research (1), 56–64.

Richter, H.J., Wallis, G.B., Charter, K.H., Murphy, S.L., 1978. Deentrainment and Countercurrent Air–water Flow in a Model PWR Hot Leg, NRC-0193-9.

Seidel, T., Vallée, C., Lucas, D., Beyer, M., Deendarlianto, 2010. Two-Phase Flow Experiments in a Model of the Hot Leg of a Pressurised Water Reactor, Wissenschaftlich-Technische Berichte/Forschungszentrum Dresden-Rossendorf; FZD-531 2010.

Siddiqui, H., Banerjee, S., Ardron, K.H., 1986. Flooding in an elbow between a vertical and a horizontal or near horizontal pipe. Part I. Experiments. International Journal of Multiphase Flow 12, 531–541.

Author's personal copy

Smits, S.R., Huang, W.D., Razi, J., Kocamustafaogullari, G., 1993. Droplet size modelling in annular flow. In: Proceeding of the 6th International Topical Meeting on Nuclear Reactor Thermal Hydraulics (NURETH-6), Grenoble, France, October 5–8, 1993.

Solmos, M., Hogan, K.J., Vierow, K., 2008. Flooding experiments and modelling for improved reactor safety. In: Proceeding of U.S. Japan Two Phase Flow Seminar, Sponsored by National Science Foundation, Hosted by UCLA College of Engineering, Santa Monica, CA, September 2008, p. 17.

Stevanovic, V., Studovic, M., 1995. A simple model for vertical annular and horizontal stratified two-phase flows with liquid entrainment and phase transitions: one-dimensional steady state conditions. Nuclear Engineering and Design 154, 357–379.

Taitel, Y., Dukler, A.E., 1976. A model for predictive flow regime transitions in horizontal and near horizontal gas–liquid flow. AICHE Journal 22, 47–55.

Tehrani, A.A.K., Patrick, M.A., Wragg, A.A., Gardner, G.C., 1990. Flooding in a scale model of the hot-leg system of a pressurized water reactor. In: Proceeding of the Winter Annual Meeting of the ASME, Dalas, TX, November, pp. 221–228.

Tye, P., 1998. Counter-Current and Flooding in Vertical and Horizontal Tubes with and without Obstructions. Ph.D. Thesis. Département de Génie Méchanique Eole Polytechnique de Montréal, Canada.

Utanohara, Y., Kinoshita, I., Murase, M., Minami, N., Tomiyama, A., 2009. Effects of interfacial friction correlations on numerical calculations for countercurrent gas–liquid flow in a PWR hot leg. In: Proceeding of the 13th International Topical Meeting on Nuclear Reactor Thermal Hydraulics (NURETH-13), Kanazawa City, Japan, September 2009.

Vallée, C., Deendarlianto, Lucas, D., Beyer, M., Pietruske, H., Carl, H., 2008. Counter-current flow limitation experiments in a model of the hot leg of a pressurised water reactor. International Journal for Nuclear Power 53 (8/9), 546–549.

Vallée, C., Deendarlianto, Beyer, M., Lucas, D., Carl, H., 2009. Air/water countercurrent flow experiments in a model of the hot leg of a pressurized water reactor. Journal of Engineering for Gas Turbines and Power – Transactions of the ASME 131, 022905.

Vallée, C., Seidel, T., Lucas, D., Tomiyama, A., Murase, M. Comparison of countercurrent flow limitation experiments performed in two different models of the hot leg of a pressurized water reactor with rectangular cross-section. Journal of Engineering for Gas Turbines and Power, in press.

Wallis, G.B., 1961. Flooding Velocities for Air and Water in Vertical Tubes. AAEW-R123, UKAEA, Harwell, England.

Wallis, G.B., 1969. One-dimensional Two-phase Flow. McGraw Hill, New York.

Wallis, G.B., Makkenchery, S., 1974. The hanging film phenomenon in vertical annular two-phase flow. Journal of Fluid Engineering (96), 297–298.

Wan, P.T., Krishnan, V.S., 1986. Air–water flooding in a 90° elbow with a slightly inclined lower leg. In: Proceeding of the Seventh Annual Conference of the Canadian Nuclear Society, Toronto, June 1986, pp. 273–278.

Wan, P.T., 1986. Countercurrent steam–water flow in an upright 90° elbow. In: Proceeding of the Eighth International Heat transfer Conference, San Francisco, CA, USA, pp. 2313–2318.

Wang, M.J., Mayinger, F., 1995. Simulation and analysis of thermal-hydraulic phenomena in a PWR hot leg related SBLOCA. Nuclear Engineering and Design 155, 643–652.

Weiss, P.A., Hertlein, R.J., 1988. UPTF test results: first three separate effect tests. Nuclear Engineering and Design 108, 249–263.

Weiss, P., Emmerling, R., Hertlein, R., Liebert, J., 1992. Two-phase flow experiments in full-scale to extend knowledge of PWR LOCA thermal-hydraulics. In: Proceeding of the National Heat Transfer Conference, San Diego, CA, USA, pp. 268–282.

Wongwises, S., 1994. Experimental investigation of two-phase countercurrent flow limitation in a bend between horizontal and inclined pipes. Experimental Thermal and Fluid Science 8, 245–259.

Wongwises, S., 1996a. Flooding in a horizontal pipe with bend – brief communication. International Journal of Multiphase Flow 22 (1), 195–201.

Wongwises, S., 1996b. Two-phase countercurrent flow in a model of a pressurized water reactor hot leg. Nuclear Engineering and Design 166, 121–133.

Zapke, K., Kroger, D.G., 2000. Countercurrent gas–liquid flow in inclined and vertical ducts. II. The validity of the Froude–Ohnesorge number correlation for flooding. International Journal of Multiphase Flow 26, p1457–p1468.